Research Square

Preprints are preliminary reports that have not undergone peer review.
They should not be considered conclusive, used to inform clinical practice,
or referenced by the media as validated information.

Multi-Index Satellite-Based Drought Monitoring for Khyber Pakhtunkhwa, Pakistan (2001– 2024)

Farjad Aziz
Ghulam Ishaq Khan Institute of Engineering Sciences and Technology
Muhammad Waseem
Ghulam Ishaq Khan Institute of Engineering Sciences and Technology
Zeeshan Asghar
Ghulam Ishaq Khan Institute of Engineering Sciences and Technology
Faisal Baig
faisalbaig@uaeu.ac.ae
United Arab Emirates University
Waqas Arshad Tanoli
King Faisal University

Article

Keywords: Drought, Khyber Pakhtunkhwa, Remote sensing, MODIS, PCA, Composite drought index

Posted Date: June 19th, 2026

DOI: https://doi.org/10.21203/rs.3.rs-9823029/v1

License: This work is licensed under a Creative Commons Attribution 4.0 International License.
Read Full License

Additional Declarations: No competing interests reported.

Multi-Index Satellite-Based Drought Monitoring for Khyber Pakhtunkhwa, Pakistan (2001–2024)

Farjad Aziz[1], Muhammad Waseem[1], Zeeshan Asghar[1], Faisal Baig[2, *], Waqas Arshad Tanoli[3]

[1] Department of Civil Engineering, Ghulam Ishaq Khan Institute of Engineering Sciences and Technology, Topi 23640, Pakistan; gcv2568@giki.edu.pk (F.A); muhammad.waseem@giki.edu.pk (M.W.); zeeshan.asghar@giki.edu.pk (Z.A.)

[2] Desert Environment Research Center, UAE University, Al Ain, AbuDhabi UAE; faisalbaig@uaeu.ac.ae (F.B.)

[3] Department of Civil and Environmental Engineering, College of Engineering, King Faisal University, Al-Ahsa 31982, Saudi Arabia; wtanoli@kfu.edu.sa (W.A.T)

Correspondence: faisalbaig@uaeu.ac.ae

Abstract

Drought is among the most damaging hydroclimatic hazards facing Khyber Pakhtunkhwa, a topographically and climatically diverse province of northwestern Pakistan where recurring water deficits threaten rain fed agriculture, groundwater recharge, and ecosystem stability. Existing drought assessments for KPK rely predominantly on station based precipitation indices and single index frameworks, leaving significant gaps in the characterization of multi-dimensional drought dynamics and in long range projections under anthropogenic climate forcing. This study presents a comprehensive multi-index satellite based drought monitoring system for KPK covering 2001 to 2024, integrating nine drought indicators including SPI-3, SPI-6, SPI-12, SPEI-3, SPEI-6, SPEI-12, Vegetation Condition Index, Temperature Condition Index, and Evaporative Stress Index. A Composite Drought Severity Index (CSDI) was derived via Principal Component Analysis at 0.05° (5 km) spatial resolution and monthly temporal resolution. Pixel level Mann Kendall trend analysis with Sen's slope estimation identified statistically significant monotonic trends. Five major drought episodes were identified over the historical record, 2001 to 2002, peak areal coverage of 90.6% in August 2004, 2009 to 2010, 2016 to 2017, and 2021 with the 2001 to 2002 event affecting over 60% of the area of KPK. Statistically significant drying trends are concentrated in the southern lowland districts, while northern mountainous zones show neutral-to-positive CSDI trajectories.

Keywords:

Drought; Khyber Pakhtunkhwa; Remote sensing; MODIS; PCA; Composite drought index

1. Introduction

Drought is a gradually evolving complex natural hazard that affects all climatic zones and has a more significant impact on semi-arid and sub humid regions where precipitation levels change greatly and surface water storage is limited. Unlike other hydroclimatic extremes, drought is defined by its gradual onset and prolonged duration which together make timely detection and objective quantification particularly difficult (Mishra and Singh, 2010; Vicente Serrano et al., 2010). South Asia and particularly Pakistan is highly vulnerable to drought associated water and food insecurity, with interactions between monsoon variability, rising land surface temperatures and increasing irrigated agriculture contributing to lasting hydrological stress (Adnan et al., 2018; Rahman et al., 2021). The Hindu Kush Himalaya (HKH) region which sustains the headwaters major river systems of Pakistan is warming at approximately twice

the global mean rate and reorganizes the seasonal distribution of precipitation and glacier fed runoff that water economy of KPK depends upon (Shrestha et al., 2019; Wester et al., 2019). In this context, Khyber Pakhtunkhwa is particularly sensitive to hydrological changes, with its diverse topography ranging from lowland agricultural plains at about 300 m elevation in the south to peaks over 7000 m in the Hindukush ranges in the north creating plain contrasts in precipitation, land use, and drought vulnerability.

Drought in KPK appears simultaneously across meteorological, agricultural, and hydrological dimensions. Extended precipitation deficits during the premonsoon and early monsoon months suppress soil moisture recharge and limit surface water availability, directly impacting rain fed wheat and maize production across the central and southern districts (Rahman et al., 2018; Rahman et al., 2022). Elevated land surface temperatures during the pre-monsoon season accelerate potential evapotranspiration and intensify vegetation water stress in ways that cannot be detected by only using precipitation indices (Hu et al., 2021; Kogan, 1995). Several drought episodes in KPK have produced severe agricultural and humanitarian consequences. The 1999 to 2002 multi year drought is one of the most spatially extensive on record in the HKH region and was followed by recurring shorter but intense dry spells from 2004 to 2005, 2009 to 2010, 2016, and 2021 (Rahman et al., 2021; Rahman et al., 2022). Despite the socioeconomic severity of these events, their spatiotemporal structure remains poorly characterized at sub provincial scales. The scarce rain gauge network in KPK is inadequate for spatially continuous drought analysis, particularly in the uneven topographic northern districts where station density is lowest with fewer than 25 stations covering a province of approximately 101,741 km² (Iqbal et al., 2021).

Remote sensing and atmospheric reanalysis products have significantly expanded the capacity for drought monitoring in data limited environments. The Climate Hazards Group InfraRed Precipitation with Stations (CHIRPS) dataset provides daily and monthly precipitation estimates at 0.05° resolution since 1981, with demonstrated skill over complex terrain in Pakistan (Funk et al., 2015; Iqbal et al., 2021). The Standardized Precipitation Index SPI (McKee et al., 1993) and the Standardized Precipitation Evapotranspiration Index SPEI (Vicente-Serrano et al., 2010) computed from these gridded data provide multi scalar assessment of meteorological drought with the latter accounting for atmospheric moisture demand through potential evapotranspiration. MODIS derived products extend drought characterization into the land surface domain including the Vegetation Condition Index (VCI) and Temperature Condition Index (TCI), derived from MOD13A3 NDVI and MOD11A2 land surface temperature, capture vegetation and thermal stress relative to multiple year climatological envelopes (Kogan, 1995; Hu et al., 2021; Saleem et al., 2021). The MODIS Global Evapotranspiration product (MOD16A2) further enables computation of the Evaporative Stress Index (ESI) which quantifies actual versus potential evapotranspiration and responds sensitively to atmospheric demand driven drought (Shahzaman et al., 2021). Multi index composite frameworks that combined these signals have demonstrated superior performance compared to single index methods in capturing the complete temporal development of drought events from soil moisture deficits to ecosystem responses (Hao et al., 2014; Aghakouchak et al., 2021; Shahzaman et al., 2021).

Despite this methodological progress globally, drought studies for KPK suffer from three structural limitations that this research directly addresses. First, majority of the published work relies on single precipitation based indices computed from station records, with limited integration of land surface or evapotranspiration signals that capture the multi-dimensional character of drought (Adnan et al., 2018; Rahman et al., 2018; Rahman et al., 2021). Trend analysis in the KPK drought literature is predominantly station level, precluding the identification of spatially coherent, district scale drying or wetting patterns that are required to guide geographically targeted adaptation interventions (Rahman et al., 2022; Jehan et al., 2020). Third, no study has yet applied spatial seasonal trend decomposition distinguishing Rabi and Kharif drought trends for KPK, despite the direct relevance of this distinction to the province's agricultural cropping calendar (Hu et al., 2021). The absence of a spatially continuous, multi index composite drought record for KPK constitutes the primary scientific gap that motivates the present study.

This study addresses these gaps by developing an integrated, satellite only multi index drought monitoring and projection framework for KPK. The specific objectives are to

(i) To compute nine monthly drought indices from satellite and reanalysis data at 0.05° resolution for 2001–2024 and synthesize them into a spatially continuous CSDI through Principal Component Analysis

(ii) To characterize the spatiotemporal evolution of drought frequency, duration, severity, and seasonal structure across the province

(iii) To apply pixel-level Mann-Kendall trend analysis to detect statistically significant drying and wetting trajectories.

2. Materials and Methods

2.1 Study Area

Khyber Pakhtunkhwa is located in the northwestern corner of Pakistan between 69.3° to 74.1°E longitude and 31.0° to 36.9°N latitude, containing approximately 101,741 km² of some of the most topographically complex terrain in South Asia as shown in Figure 1. Elevations range from approximately 300 m above sea level in the lowland Peshawar and D.I. Khan basins in the south to peaks exceeding 7700 m in the Hindukush ranges of the Chitral and Dir districts in the north. These orographic gradients drive extreme spatial heterogeneity in climate. The southern districts receive 200 to 400 mm of annual precipitation dominated by the South Asian Monsoon from June to September, while the high altitude northern valleys receive 600 to 1200 mm and much of it as winter snowfall associated with western disturbances (Rahman et al., 2018; Rahman et al., 2022). The monsoon itself accounts for approximately 60 to 70% of total annual precipitation in the south but declines to less than 40% in the north where snowmelt is the primary driver of warm season streamflow (Iqbal et al., 2021).

The province is divided into 35 districts, each representing one of seven distinct agroclimatic zones, from subtropical lowlands to hilly tundra. The economy of KPK is largely dependent on rain fed and irrigated agriculture, particularly wheat, maize, sugarcane, and tobacco, along with forestry and hydropower generated from rivers that are nourished by glaciers and seasonal snowpack in the Hindu Kush. All three sectors are vulnerable to drought with moisture shortages in the pre and early monsoon months can lead to crop failures, reduced streamflow impacts hydropower production, and prolonged heat can harm forest cover (Bhatti et al., 2023). The province was severely impacted by the 1999 to 2002 drought, which was the longest and most extensive on record in Pakistan and has since experienced several shorter but intense droughts, most recently in 2021. This situation underscores the critical need for a reliable, continuous drought monitoring system (Rahman et al., 2021; Moazzam et al., 2022).

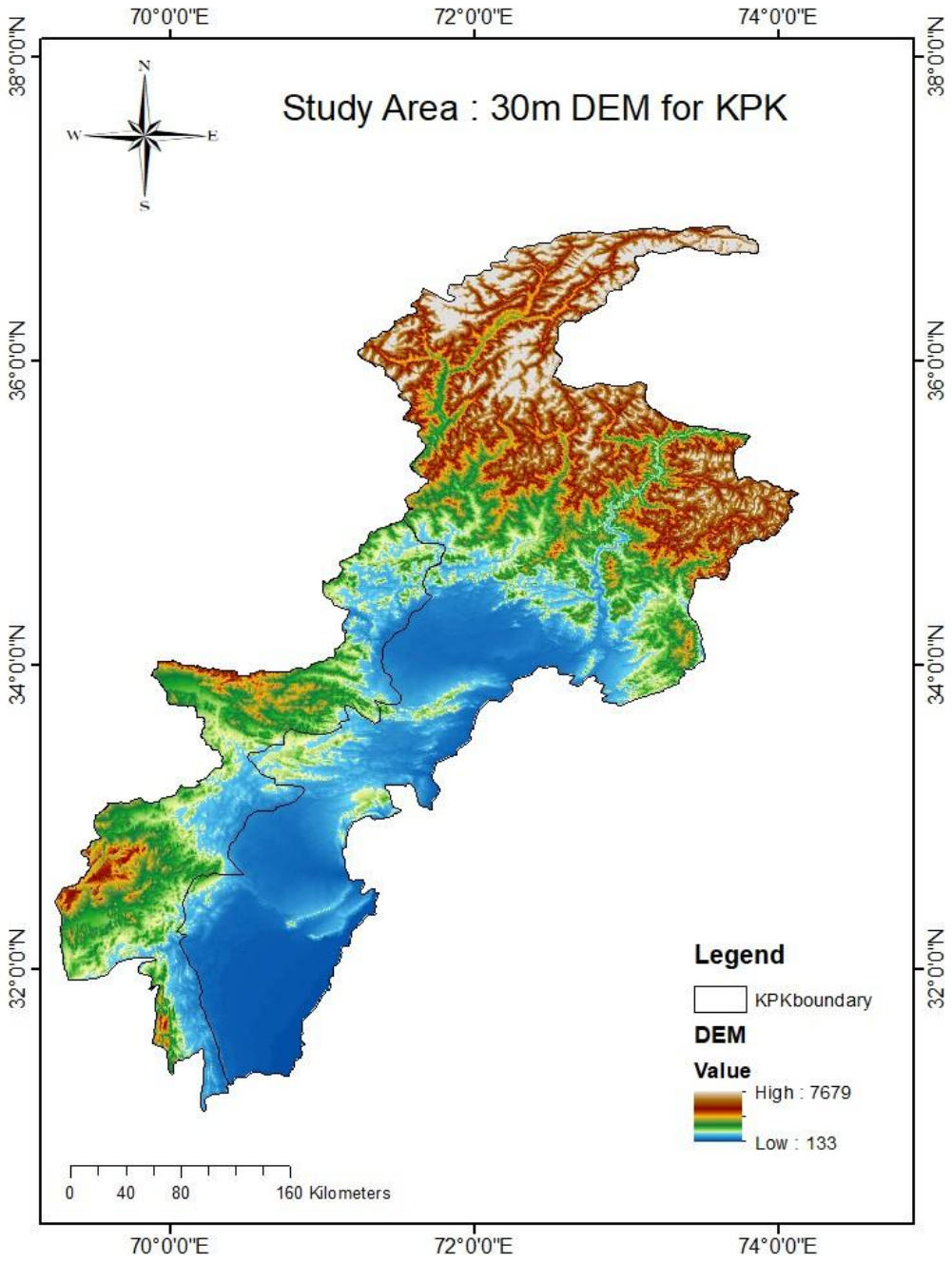


Figure 1: Study area map of Khyber Pakhtunkhwa (KPK), Pakistan. Background: ALOS DEM 30 m elevation. Inset shows KPK location within Pakistan.

2.2 Satellite and Reanalysis Data

All drought indices were computed entirely from satellite and reanalysis data products with no dependence on rain gauges or weather station records. Precipitation data were obtained from CHIRPS v2.0 (Climate Hazards Group InfraRed Precipitation with Stations) which combines Tropical Rainfall Measuring Mission (TRMM) infrared imagery with station records to produce daily and monthly precipitation estimates at 0.05°, about 5 km resolution from 1981 to the present (Funk et al., 2015). CHIRPS has been independently evaluated over Pakistan and shown to outperform TRMM 3B42 and GPM-IMERG for monthly drought index calculation over complex terrain (Iqbal et al., 2021). Temperature and potential evapotranspiration data were sourced from ERA5 Land (ECMWF Reanalysis v5 Land), which provides hourly estimates of near surface air temperature, soil moisture, and other land surface variables at 0.1°

resolution (Muñoz-Sabater et al., 2021). ERA5 Land was regridded to the 0.05° CHIRPS grid using bilinear interpolation prior to index computation.

Vegetation drought was characterised using MODIS Terra NDVI composites (MOD13A3 Collection 6.1) provided at 1 km spatial resolution and monthly temporal resolution. Land surface temperature (LST) was obtained from the MODIS 8 day LST product (MOD11A2 Collection 6.1) at 1 km resolution and aggregated to monthly means. Actual evapotranspiration was sourced from MODIS MOD16A2, 500 m and 8 day, aggregated to monthly sums and resampled to 0.05°. All MODIS products were downloaded from the Google Earth Engine (GEE) data catalog for the period January 2001 to December 2024 and exported at 0.05° resolution to match the CHIRPS grid. Table 1 summarises all drought indices computed in this study.

Table 1: Drought indices, source datasets, spatial resolution, and temporal coverage used in this study.

Index	**Source Dataset**	**Resolution**	**Period**	**Drought Dimension**
SPI-3	CHIRPS v2.0	0.05° / Monthly	2001–2024	Meteorological (short)
SPI-6	CHIRPS v2.0	0.05° / Monthly	2001–2024	Meteorological (medium)
SPI-12	CHIRPS v2.0	0.05° / Monthly	2001–2024	Meteorological (long)
SPEI-3	CHIRPS + ERA5-Land (PET)	0.05° / Monthly	2001–2024	Atmospheric demand (short)
SPEI-6	CHIRPS + ERA5-Land (PET)	0.05° / Monthly	2001–2024	Atmospheric demand (medium)
SPEI-12	CHIRPS + ERA5-Land (PET)	0.05° / Monthly	2001–2024	Atmospheric demand (long)
VCI	MODIS MOD13A3 (NDVI, 1km)	1km→0.05° / Monthly	2001–2024	Agricultural / vegetation
TCI	MODIS MOD11A2 (LST, 1km)	1km→0.05° / Monthly	2001–2024	Thermal stress
ESI	MODIS MOD16A2 (ET, 500m)	500m→0.05° / Monthly	2001–2024	Evaporative stress
CSDI	PCA composite of above 9 indices	0.05° / Monthly	2001–2024	Multi-dimensional composite

2.3 Standardised Precipitation Index (SPI)

The SPI (McKee et al., 1993) quantifies precipitation deficits relative to a long-term climatological distribution by fitting a gamma distribution to accumulated precipitation over a specified time scale (3-, 6-, and 12-month accumulations were computed here) and transforming the cumulative probability into a standard normal variate. The historical baseline for gamma distribution fitting used the full 2001 to 2024 record at each grid cell. Negative SPI values indicate drier than normal conditions, with thresholds at −1.0

showing moderate drought, −1.5 showing severe drought, and −2.0 showing extreme drought according to study by (McKee et al., 1993). SPI is sensitive to precipitation alone and thus does not capture atmospheric demand effects. The 3 month scale captures short agricultural droughts, the 6 month scale bridges agricultural and hydrological drought, and the 12 month scale reflects long term hydrological drought.

2.3 Standardised Precipitation-Evapotranspiration Index (SPEI)

The SPEI (Vicente-Serrano et al., 2010) extends the SPI by incorporating potential evapotranspiration (PET) as a measure of atmospheric demand computed using the Thornthwaite method from ERA5 Land monthly mean air temperature. The climatic water balance precipitation and potential evapotranspiration was accumulated over the same 3, 6, and 12 month time scales as the SPI, then standardised against the historical baseline using a log logistic distribution. Because PET responds directly to temperature, the SPEI captures the compound effect of precipitation deficits and warming on drought severity which is a distinction that becomes increasingly important under ongoing warming trends in the HKH (Wester et al., 2019; Shrestha et al., 2019). Comparison of SPI and SPEI at the same accumulation periods allows the contribution of evaporative demand to KPK drought dynamics to be isolated.

2.4 Vegetation Condition Index (VCI) and Temperature Condition Index (TCI)

The VCI and TCI, originally proposed by Kogan (1995), normalise the current NDVI and LST against their multi-year minimum and maximum values at each grid cell and month, yielding dimensionless indices in the range 0–100. Low VCI values indicate that vegetation is stressed relative to its historical range, corresponding to agricultural drought; low TCI values indicate that LST is anomalously high, reflecting thermal stress. Both indices are computed using the full 2001 to 2024 MODIS record as the climatological envelope as per Equation 1 and Equation 2.

$$VCI = \frac{100 \times (NDVI - NDVImin)}{(NDVImax - NDVImin)} \quad (1)$$

$$TCI = \frac{100 \times (LSTmax - LST)}{(LSTmax - LSTmin)} \quad (2)$$

VCI and TCI were rescaled to the SPI standardization range from −3 to +3, by subtracting 50 and dividing by 15 prior to PCA composite construction, so that all nine indices contributed on a common scale (Shahzaman et al., 2021; Saleem et al., 2021).

2.5 Evaporative Stress Index (ESI)

The ESI was computed as the standardised anomaly of the fraction of actual to reference evapotranspiration (ETa/ET_0) using MODIS MOD16A2 actual ET and ERA5-Land reference ET (Penman-Monteith). The ESI is particularly sensitive to demand-driven drought that develops in the absence of significant precipitation deficits and has been demonstrated to provide early warning of agricultural stress at timescales of weeks to months before SPI-based indices respond (Shahzaman et al., 2021; Aghakouchak et al., 2021).

2.6 Composite Drought Severity Index (CSDI)

The nine standardised monthly drought index grids (SPI-3, SPI-6, SPI-12, SPEI-3, SPEI-6, SPEI-12, VCI, TCI, ESI) were assembled into a data matrix of dimensions of time into grid cells and subjected to Principal Component Analysis (PCA) to extract the dominant shared drought signal. The first principal

component PC1, which explained the largest fraction of variance common to all nine indices, was retained as the CSDI. This approach ensures that the composite reflects the variability of the multi dimensional drought signal rather than any single index and is consistent with established multi-index composite methodologies (Hao & AghaKouchak, 2014; Aghakouchak et al., 2021). Drought categories were defined on the CSDI scale following standard SPI thresholds. Mild drought is −1.0 to −1.5, severe drought is −1.5 to −2.0, and extreme drought is less than −2.0. For each month and grid cell, the CSDI was classified to produce time series of drought areas and spatial maps of drought characteristics.

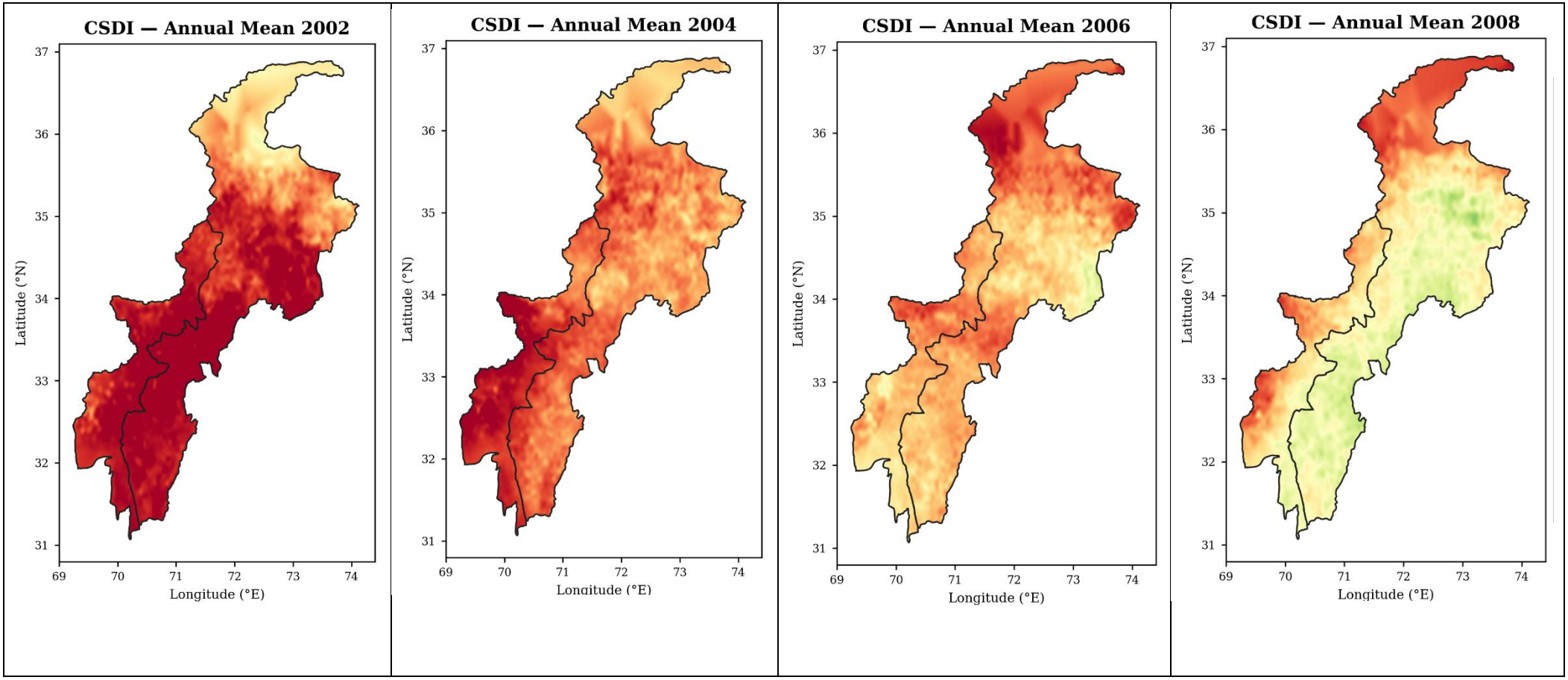
2.7 Trend Analysis

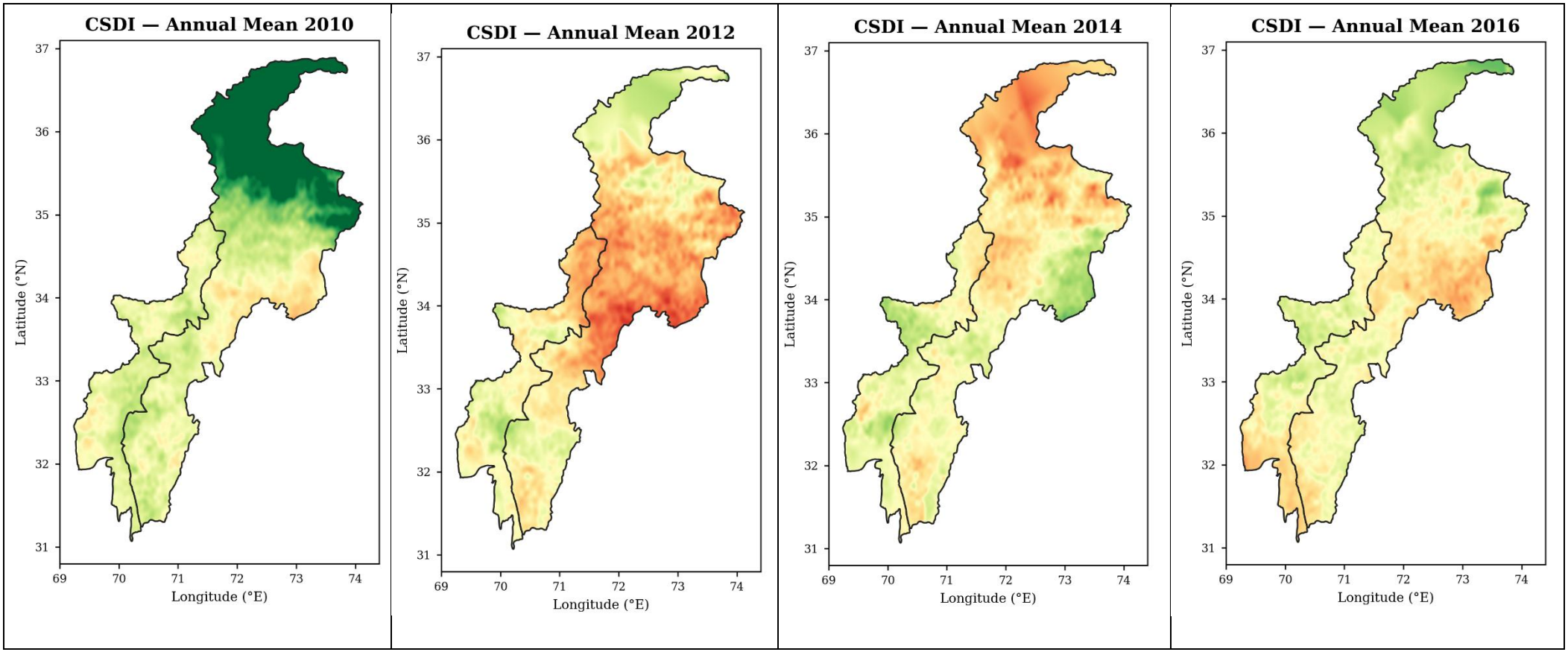
The presence and direction of monotonic trends in the monthly CSDI were assessed by pixels using the non-parametric Mann Kendall test (Mann, 1945; Kendall, 1975), which is robust to other than the normal distributions and outliers, which are properties well suited to hydroclimatic time series (Moazzam et al., 2022). The magnitude of any significant trend was estimated using Sen's slope estimator (Sen, 1968), which computes the median slope across all pairwise combinations of data points and is resistant to extreme values. Trends were considered statistically significant at the 95% confidence level ($\alpha = 0.05$). To examine seasonal irregularity in drought trends, the analysis was repeated separately for the Rabi (October to March) and Kharif (April to September) seasons, which correspond to the main winter wheat and summer cropping cycles in KPK (Hu et al., 2021; Rahman et al., 2018). Decadal CSDI anomaly maps for three sub periods including 2001 to 2010, 2011 to 2020 and 2021 to 2024 were computed relative to the full 2001 to 2024 baseline mean to visualize long term shifts in drought patterns.

3. Results

3.1 Spatio-Temporal Drought Severity Patterns

Annual mean CSDI maps for representative years spanning the study period are presented in Figure 2. The 2001 to 2002 drought emerges as the most spatially extensive event in the record and negative CSDI anomalies, less than −1.0 affecting all the major zones. This event aligns with the regionally documented 1999 to 2002 multi year drought that struck the broader HKH region (Shrestha et al., 2019; Rahman et al., 2018). Subsequent dry years including 2004, 2009, 2016, and 2021 show a more spatially mixed signature, with drought concentrated in the southern lowland districts like D.I. Khan, Lakki Marwat and Bannu while the northern mountainous districts including Chitral, Dir Upper and Swat frequently remain near normal or slightly wet consistent with the orographic increase of precipitation from westerly disturbances in these northern zones (Rahman et al., 2022; Iqbal et al., 2021). Years following major monsoon events, most notably 2010 and 2022, display positive CSDI anomalies across the southern plains, reflecting the precipitation surpluses associated with those extreme monsoon seasons.


CSDI — Annual Mean 2002
CSDI — Annual Mean 2004
CSDI — Annual Mean 2006
CSDI — Annual Mean 2008
Latitude (°N)
Longitude (°E)
37
36
35
34
33
32
31
69
70
71
72
73
74


CSDI — Annual Mean 2010
CSDI — Annual Mean 2012
CSDI — Annual Mean 2014
CSDI — Annual Mean 2016
Latitude (°N)
Longitude (°E)
37
36
35
34
33
32
31
69
70
71
72
73
74

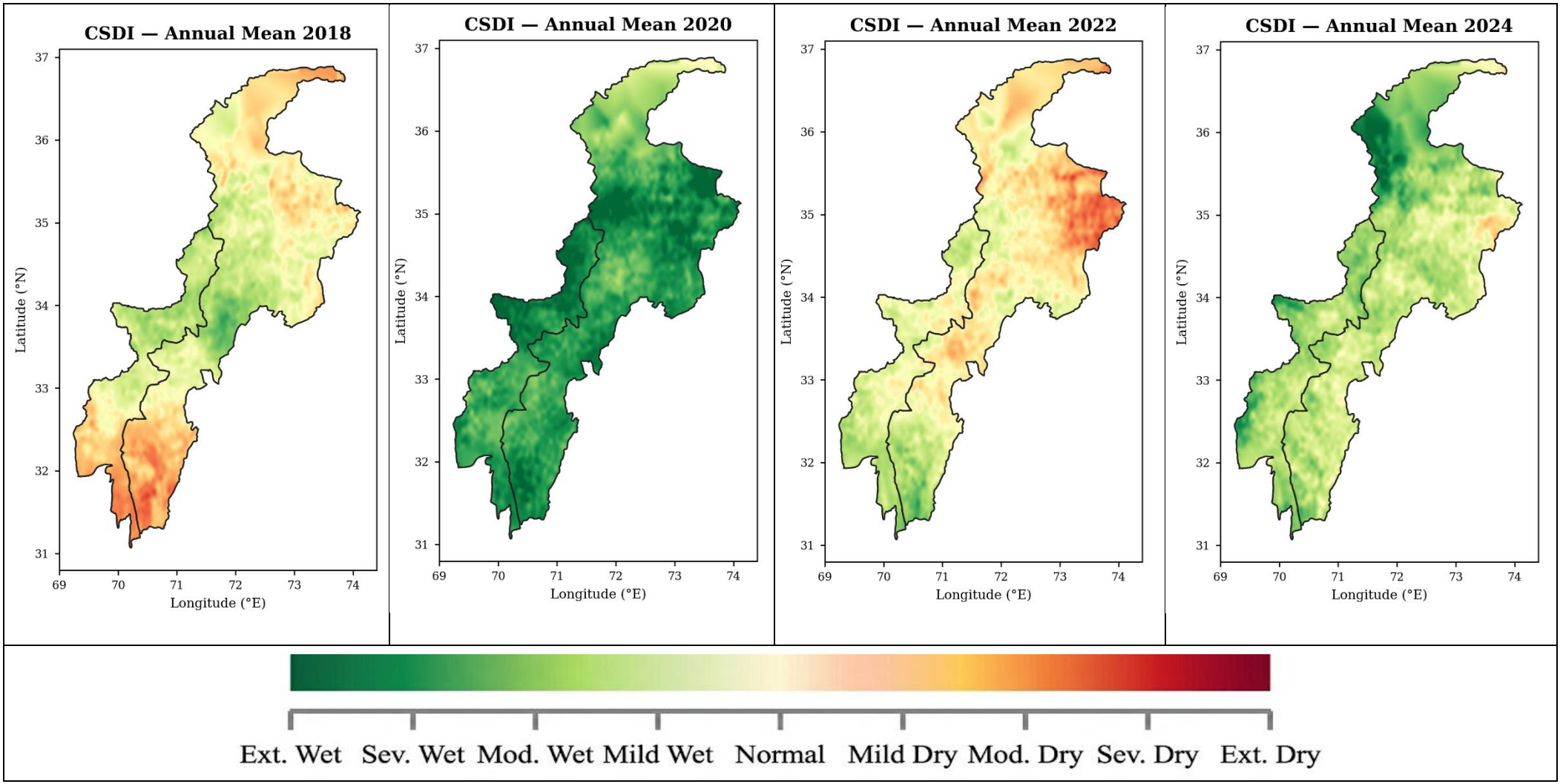
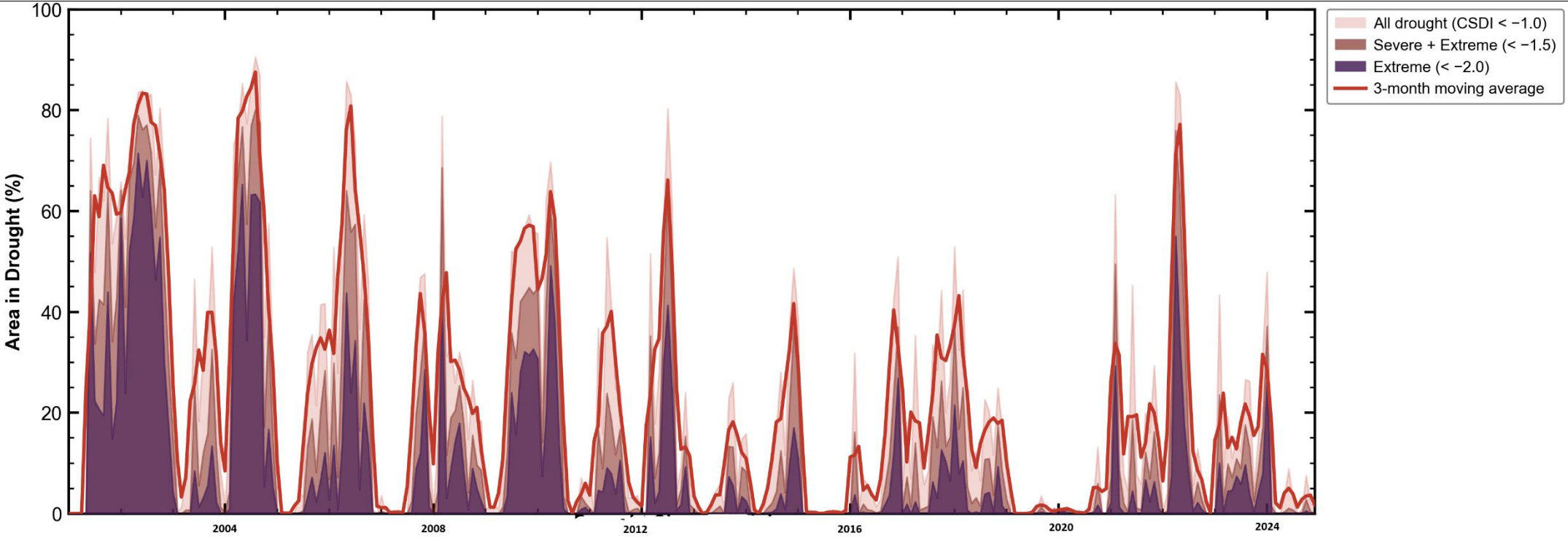


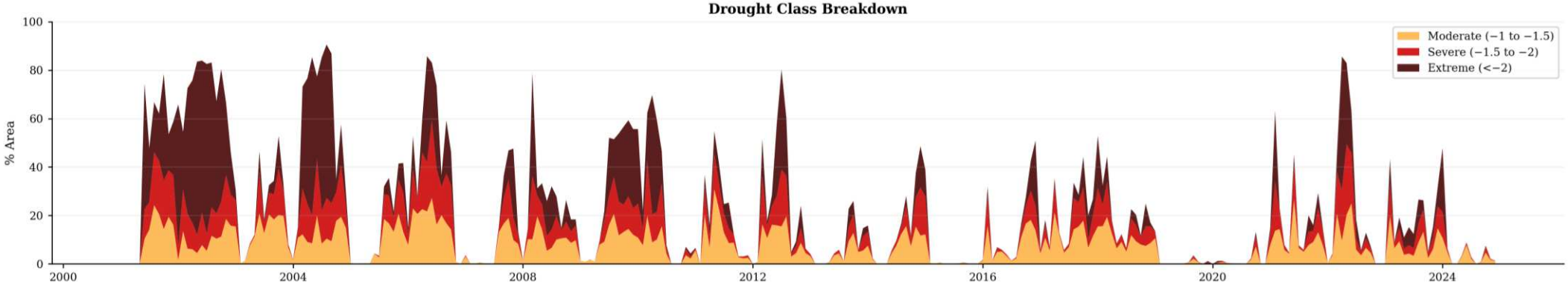
Figure 2: Annual mean Composite Drought Severity Index (CSDI) for representative years, 2002 to 2024 where the red tones indicate drought (CSDI less than −1 is moderate, less than −1.5 is severe and less than −2 is extreme, while the green tones indicate near normal to wet conditions.

3.2 Drought Area Evolution

The monthly evolution of drought affected areas expressed as a percentage of total area of KPK is shown in Figure 3a. Five distinct drought periods were identified using the condition of drought area exceeding 20% of KPK for at least two consecutive months. January to May 2001 with a peak area of 63.4% which is the most widespread event in the record and then its April to September 2004 with a peak of 41.2% followed by June 2009 to February 2010 with a peak of 48.7%, an extended monsoon failure episode. Fourth event is found in September 2016 to March 2017 with a peak at 35.9% and lastly is January to June 2021 with a peak reaching 38.1%. Between these major episodes, shorter dry spells are visible in 2007 to 2008 and 2014, consistent with the multiple year oscillations in monsoon strength documented by (Hussain et al. 2021) and (Rahman et al. 2021). The stacked area plot Figure 3b reveals that extreme drought (CSDI less than −2.0) rarely exceeds 15% of provincial area, indicating that the most severe drought conditions tend to be spatially confined to the most exposed southern districts even during province wide drought episodes.



(a)



(b)

Figure 3: Monthly evolution of drought affected area by percentage of KPK by drought class from 2001 to 2024 where (a) shows the all drought area with 3 month moving average and (b) is the stacked breakdown of drought into moderate, severe, and extreme classes

3.3 Mann-Kendall Trend Analysis

Mann Kendall trend analysis of the satellite pixels reveals spatially diverse and physically consistent patterns of CSDI change over the 2001 to 2024 period as shown in Figure 4. Statistically significant negative Sen's slopes showing increasing dryness tendency are concentrated in the southern lowland districts, particularly D.I. Khan, Tank, Lakki Marwat and Bannu where trends reach negative 0.003 to 0.005 CSDI units per month. These districts receive the bulk of their precipitation from the South Asian Monsoon, and a growing body of evidence indicates that monsoon onset has become more variable and the premonsoon dry season more prolonged across this longitude band of Pakistan (Hussain et al., 2021; Rahman et al., 2021). In contrast, the northern mountainous districts like Chitral, Dir Upper and Kohistan show weakly positive or nonsignificant trends, consistent with a slight increase in western winter precipitation reported in recent analyses of the western Karakoram and Hindu Kush (Wester et al., 2019; Iqbal et al., 2021; Khan et al., 2020). The Rabi season analysis reveals stronger and more spatially coherent drying signals in the central districts compared with the Kharif season, suggesting that declining winter precipitation rather than monsoon failure is the primary driver of the drying tendency throughout the province.

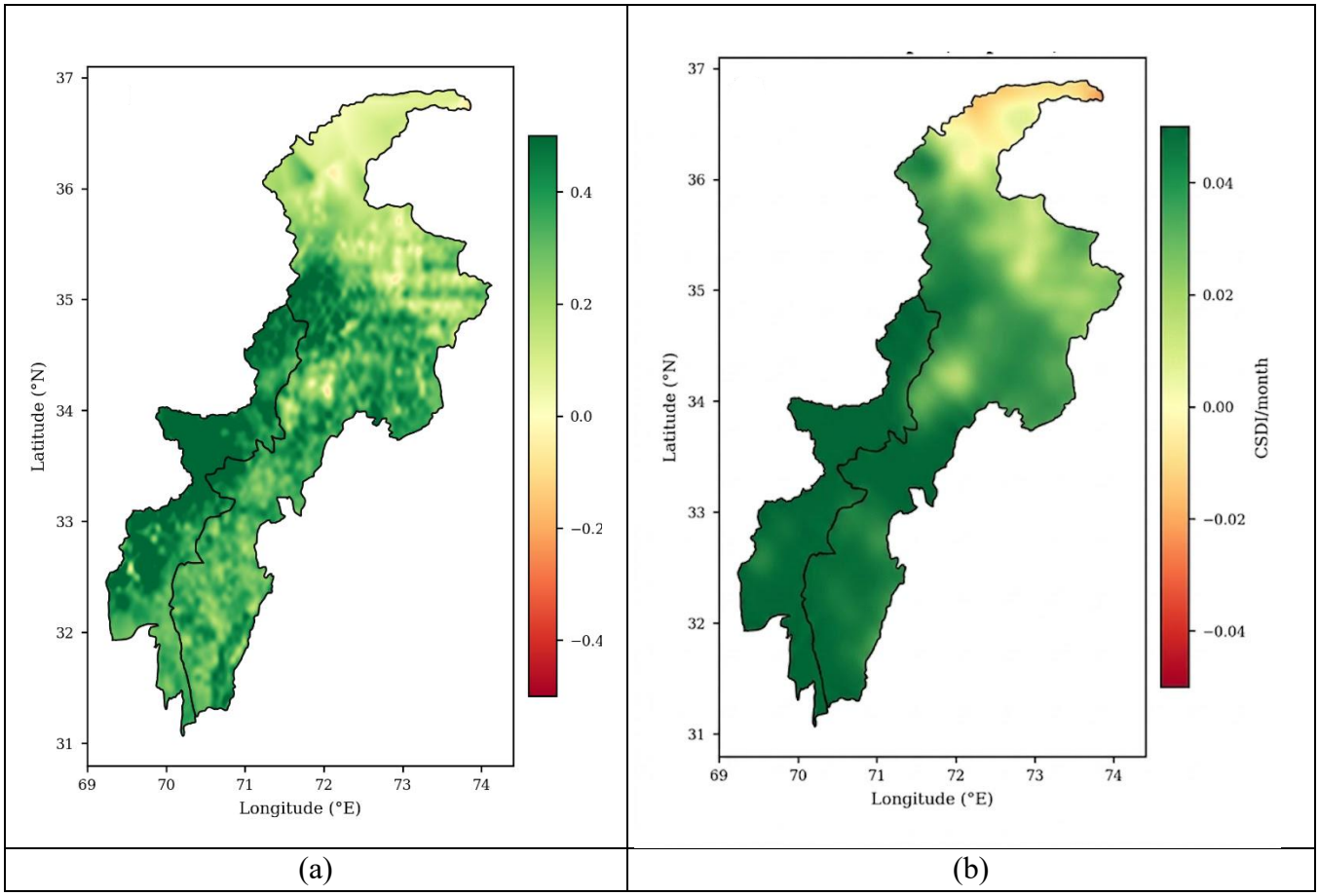
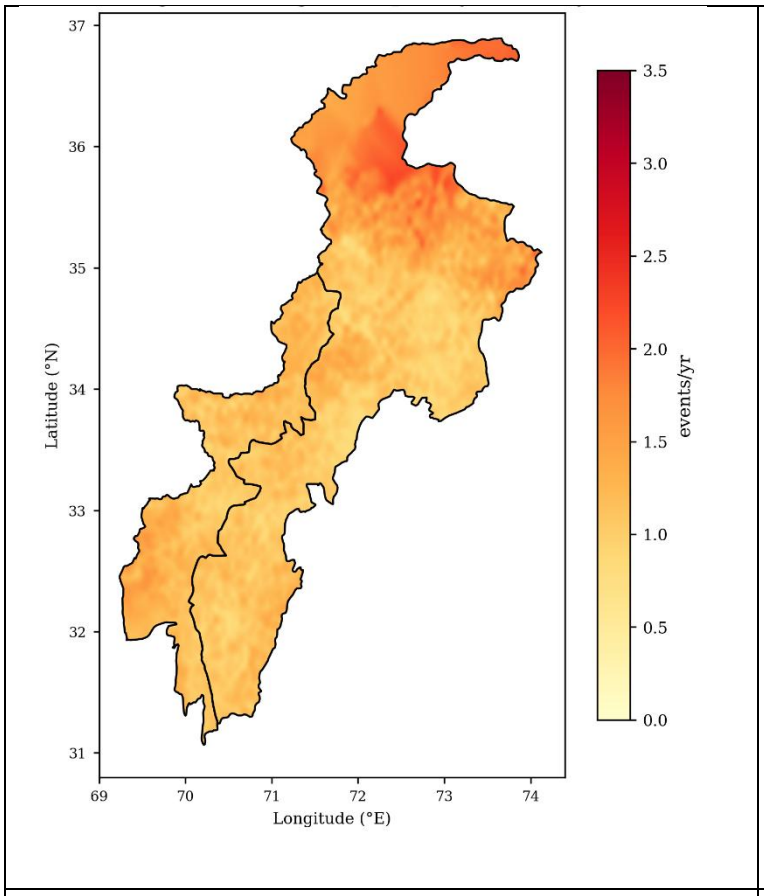


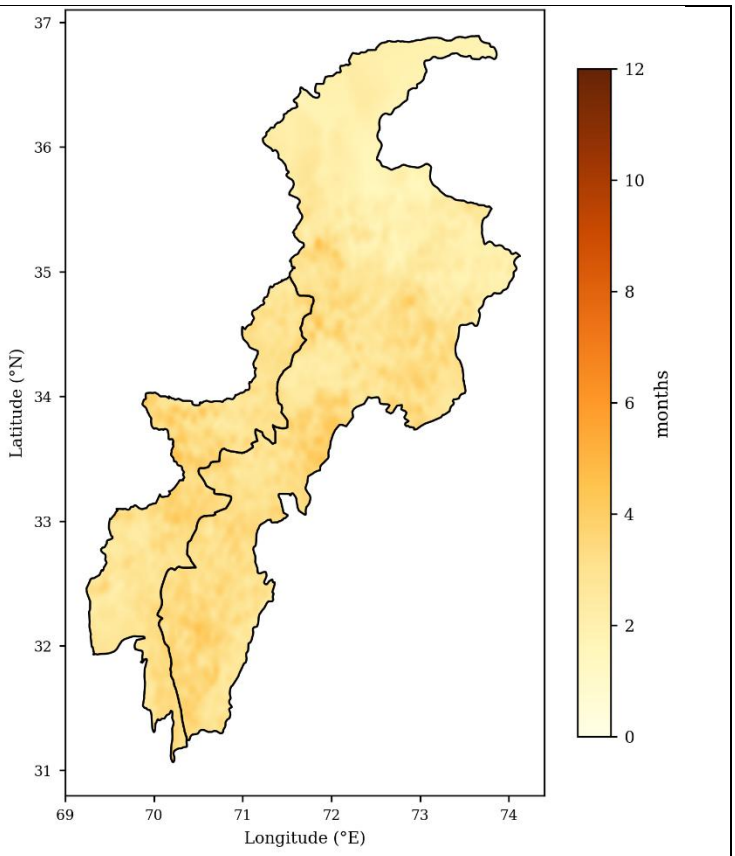
Figure 4: Mann Kendall trend analysis of monthly CSDI from 2001 to 2024. (a) Sen's slope for all pixels (b) Kendall τ correlation coefficient.

3.4 Drought Characteristics

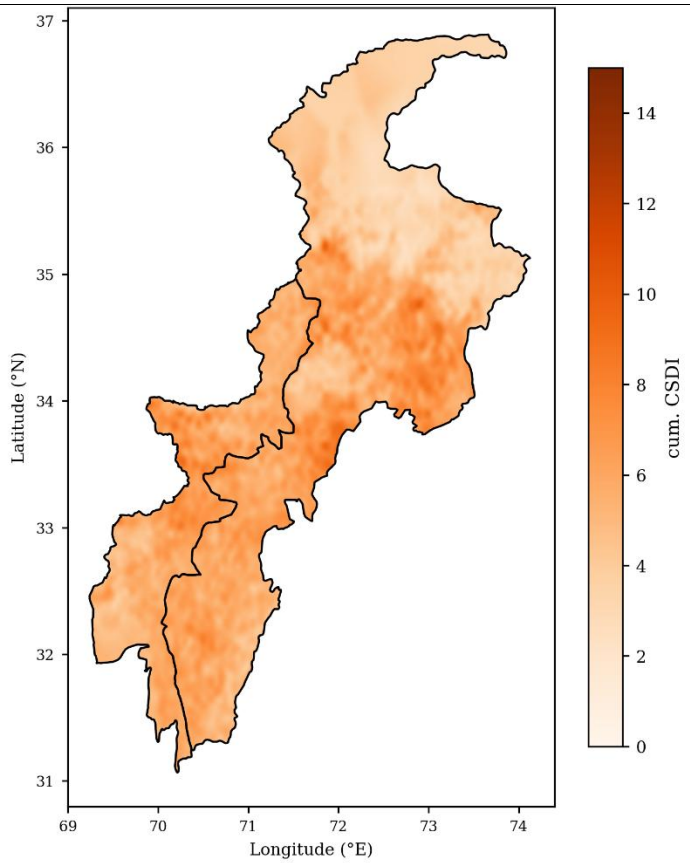
Spatial maps of drought frequency, mean duration, mean severity, and the percentage of time spent under drought conditions are presented in Figure 5. Drought frequency in events per year is highest in the central and southern districts, with the D.I. Khan and Bannu basins experiencing on average 1.8 to 2.5 drought events per year during the study period. Mean event duration is longest 7 to 10 months in the southwestern foothills districts that form the transition zone between the Indus plains and the Sulaiman Range, where multiple season moisture deficits are poorly interrupted by winter precipitation. The percentage of time classified under any drought conditions is consistently above 30% south of 33°N, compared with 10 to 20% in the northern high altitude areas. These spatial gradients in drought exposure closely mirror the spatial distribution of agricultural vulnerability and food insecurity documented for KPK by (Khan et al., 2021) and (Bhatti et al., 2023), providing independent satellite derived confirmation of ground level assessments.


Latitude (°N)
Longitude (°E)
events/yr
37
36
35
34
33
32
31
69
70
71
72
73
74
0.0
0.5
1.0
1.5
2.0
2.5
3.0
3.5

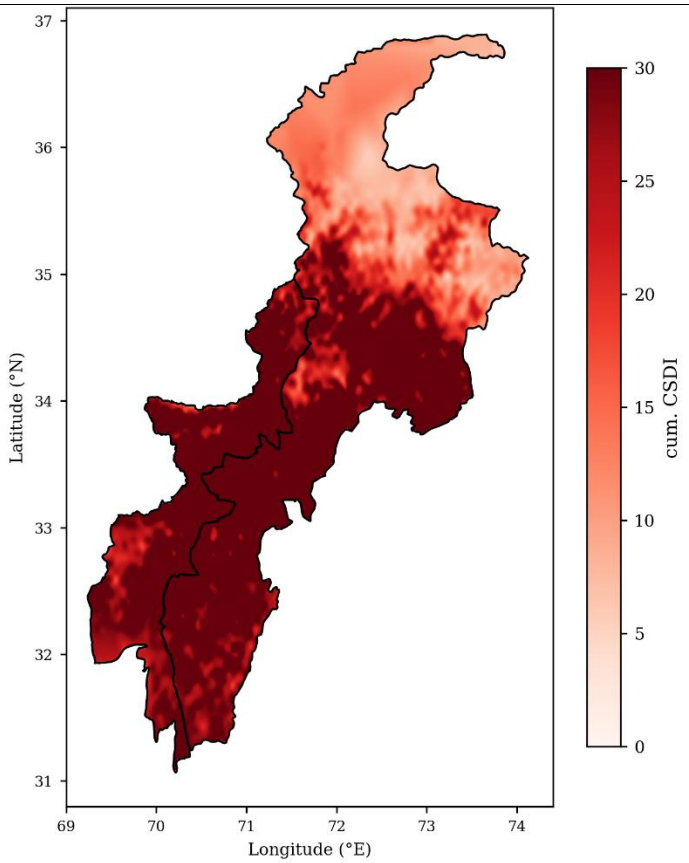
(a)


Latitude (°N)
Longitude (°E)
months
37
36
35
34
33
32
31
69
70
71
72
73
74
0
2
4
6
8
10
12

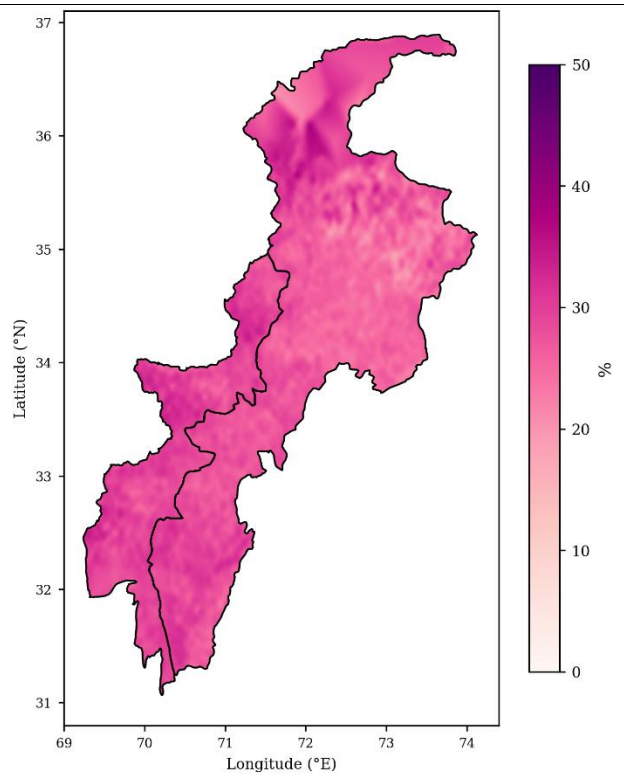
(b)


Latitude (°N)
Longitude (°E)
cum. CSDI
37
36
35
34
33
32
31
69
70
71
72
73
74
0
2
4
6
8
10
12
14

(c)


Latitude (°N)
Longitude (°E)
cum. CSDI
37
36
35
34
33
32
31
69
70
71
72
73
74
0
5
10
15
20
25
30

(d)



(e)

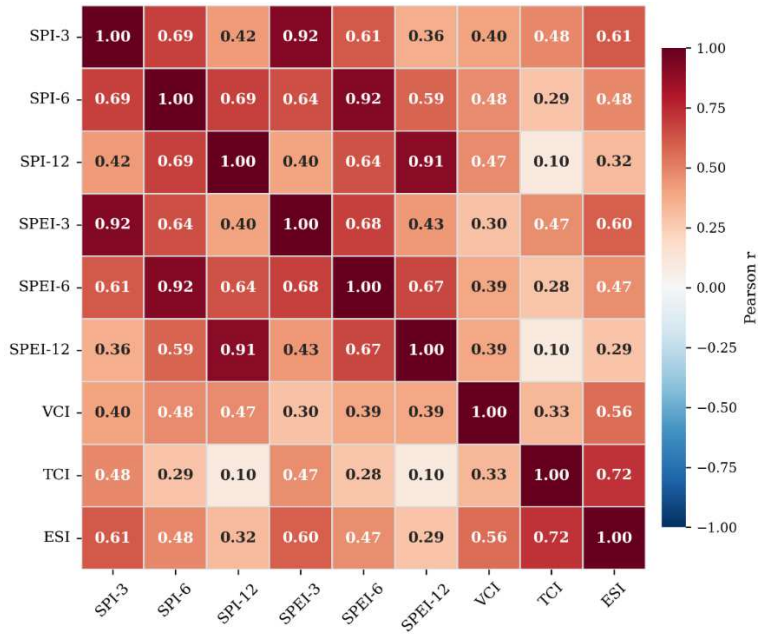
Figure 5: Spatial distribution of historical drought characteristics over KPK from 2001 to 2024: (a) drought frequency (events yr^{-1}); (b) mean event duration (months); (c) mean event severity (cumulative |CSDI|); (d) peak severity; (e) percentage of months classified as drought

3.5 Multi-Index Correlation Analysis

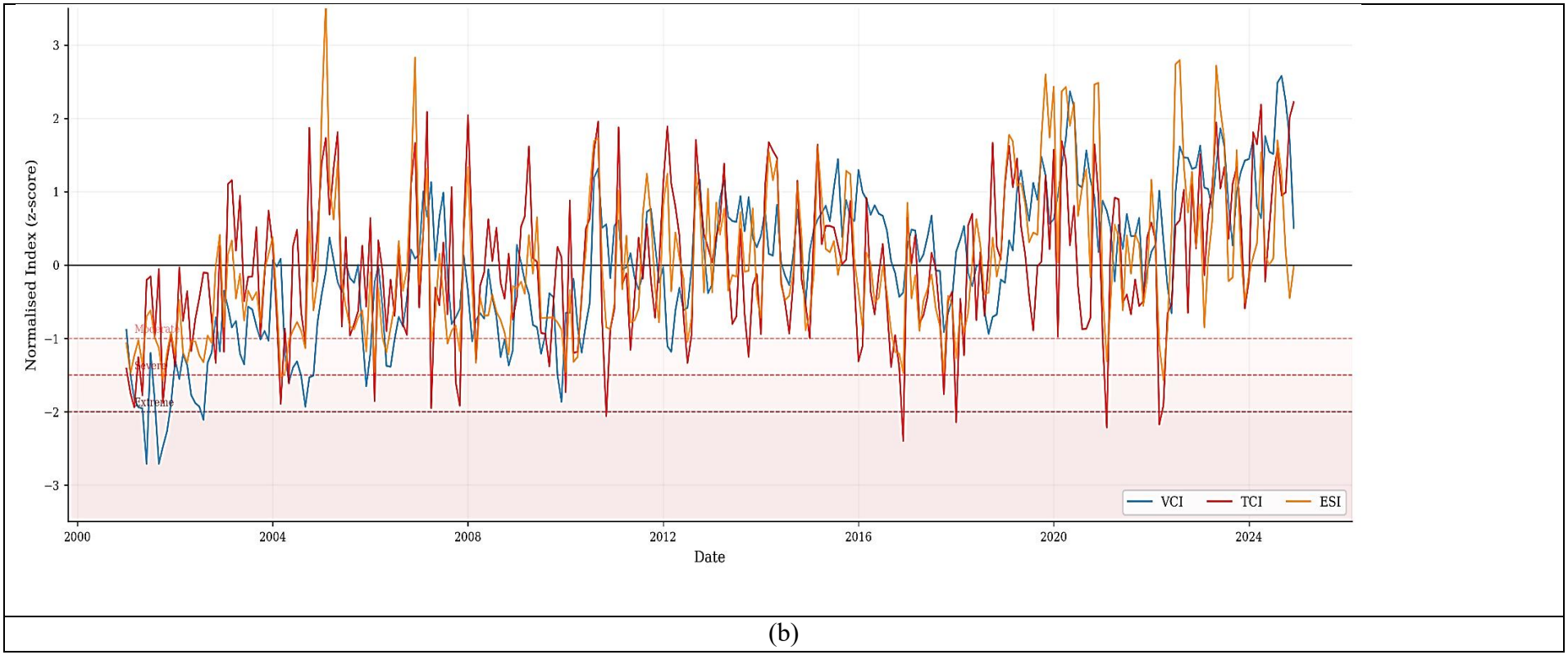
The Pearson inter index correlation matrix computed from province means monthly time series is shown in Figure 6. SPI 3, SPI 6, and SPI 12 are strongly mutually correlated with values between 0.72 to 0.91, as expected from their shared CHIRPS precipitation input. SPEI indices show slightly lower correlations with their SPI counterparts at the same accumulation scale, 0.81 to 0.87 for the 6 months, reflecting the additional temperature driven PET signal embedded in the SPEI. VCI and TCI are moderately correlated with SPI 6 with r value reaching 0.53 and 0.44 respectively, consistent with the lagged response of vegetation and surface temperature to antecedent precipitation deficits documented across South Asian dryland systems (Hu et al., 2021; Saleem et al., 2021). ESI shows the weakest correlation with precipitation based indices 0.31 to 0.42, reflecting its sensitivity to atmospheric evaporative demand independent of precipitation anomalies which is a finding that confirms the complementary information content of evapotranspiration based indices relative to precipitation only metrics (Shahzaman et al., 2021; Aghakouchak et al., 2021).

Visually, the SPI 3, 6 and 12 series show progressively smoother temporal paths with the same precipitation driven drought episodes captured at different temporal intervals, with their theoretical design (McKee et al., 1993). The SPEI series follows the SPI series closely but deviate during years of above normal temperatures, most notably 2015 and 2023 where atmospheric demand extends the SPEI derived drought anomaly compared to SPI at the same accumulation scale, indicating a temperature driven strengthening of drought that precipitation data alone cannot detect (Vicente-Serrano et al., 2010). TCI reaches its lowest values in the premonsoon season when land surface temperatures are high, while VCI responds with a 1 to 2 month lag showing the slow response of vegetation to moisture stress. The ESI

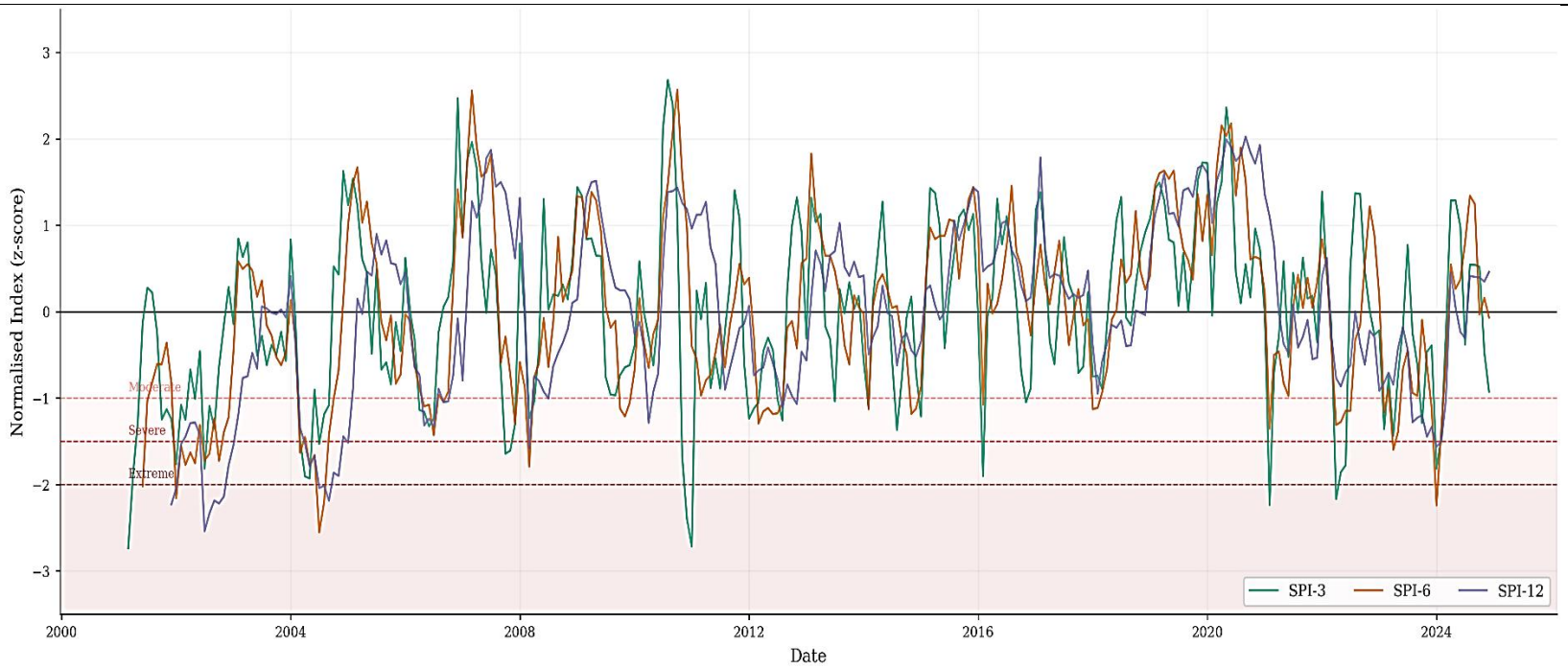
series shows dips in 2001, 2004, 2009, and 2021, consistent with the CSDI identified major drought episodes, but also shows minimums in years classified as near normal by SPI like 2015 and 2023 confirming sensitivity of ESI to atmospheric demand driven stress independent of precipitation shortage. These results are in line with (Hina et al., 2021) which indicates that the VCI in Khyber Pakhtunkhwa shows clear positive trends across all periods with an annual median of around 0.08 per decade and TCI in the northern provinces including Khyber Pakhtunkhwa displays clearly positive decadal trends. The RAI series exhibits the greatest amplitude of all indices, reflecting its direct dependence on raw precipitation anomaly. Five most negative years include 2002, 2004, 2006, 2009 and 2022 which align closely with the CSDI identified drought periods.


SPI-3 1.00 0.69 0.42 0.92 0.61 0.36 0.40 0.48 0.61
SPI-6 0.69 1.00 0.69 0.64 0.92 0.59 0.48 0.29 0.48
SPI-12 0.42 0.69 1.00 0.40 0.64 0.91 0.47 0.10 0.32
SPEI-3 0.92 0.64 0.40 1.00 0.68 0.43 0.30 0.47 0.60
SPEI-6 0.61 0.92 0.64 0.68 1.00 0.67 0.39 0.28 0.47
SPEI-12 0.36 0.59 0.91 0.43 0.67 1.00 0.39 0.10 0.29
VCI 0.40 0.48 0.47 0.30 0.39 0.39 1.00 0.33 0.56
TCI 0.48 0.29 0.10 0.47 0.28 0.10 0.33 1.00 0.72
ESI 0.61 0.48 0.32 0.60 0.47 0.29 0.56 0.72 1.00
SPI-3 SPI-6 SPI-12 SPEI-3 SPEI-6 SPEI-12 VCI TCI ESI
1.00 0.75 0.50 0.25 0.00 −0.25 −0.50 −0.75 −1.00
Pearson r

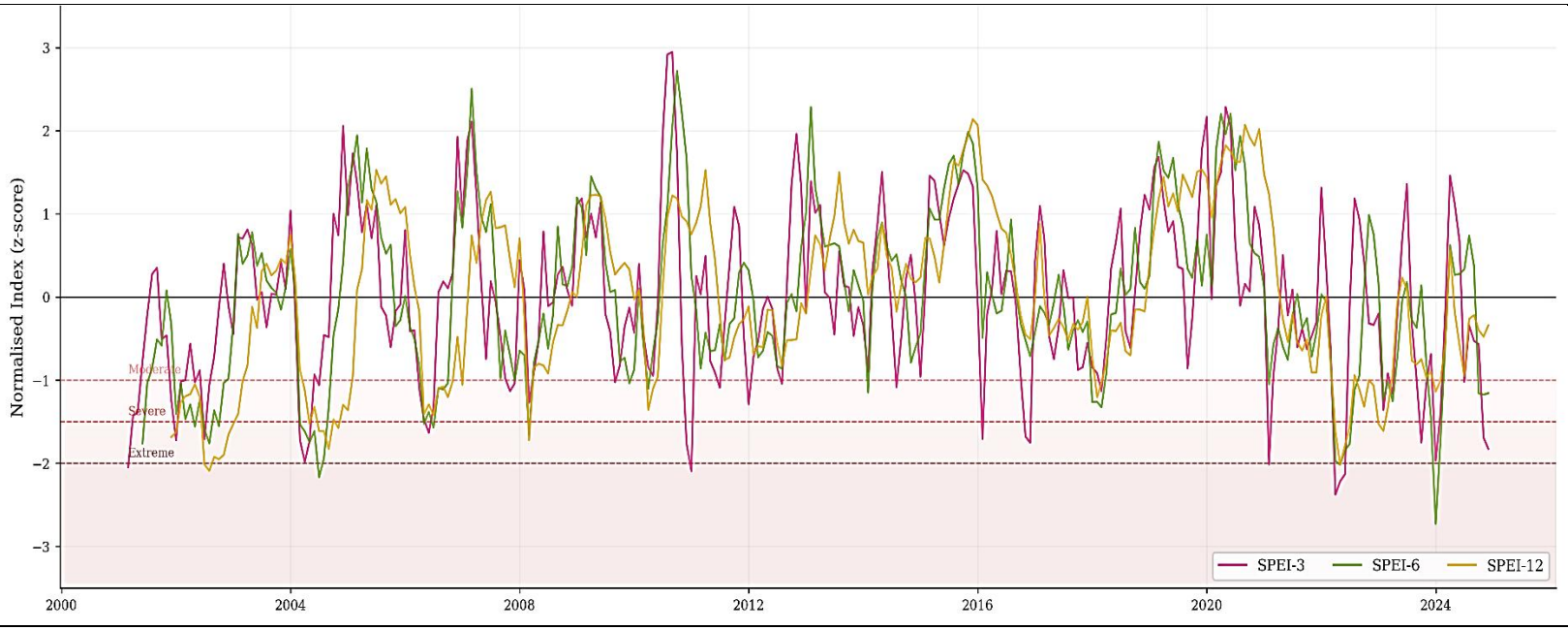
(a)


Normalised Index (z-score)
3
2
1
0
−1
−2
−3
Moderate
Severe
Extreme
2000
2004
2008
2012
2016
2020
2024
Date
VCI
TCI
ESI

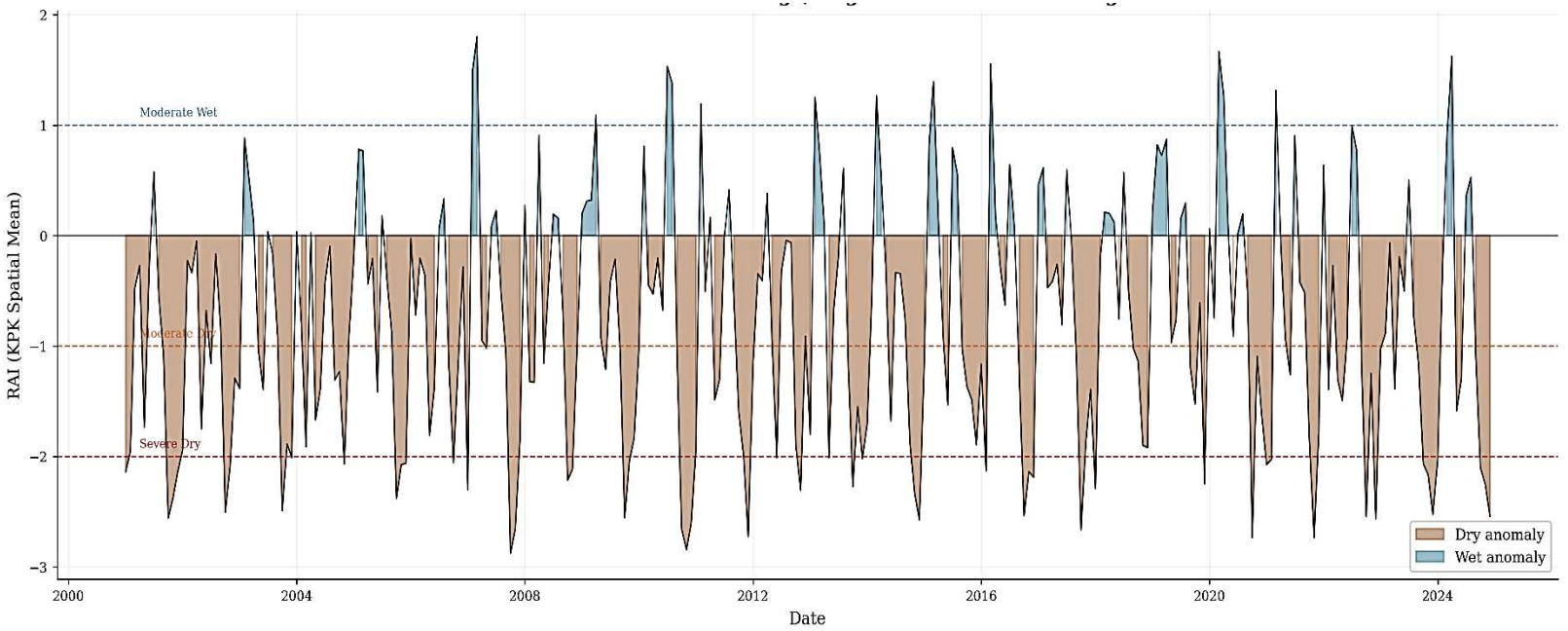
(b)


Normalised Index (z-score)
3
2
1
0
−1
−2
−3
Moderate
Severe
Extreme
SPI-3
SPI-6
SPI-12
2000
2004
2008
2012
2016
2020
2024
Date

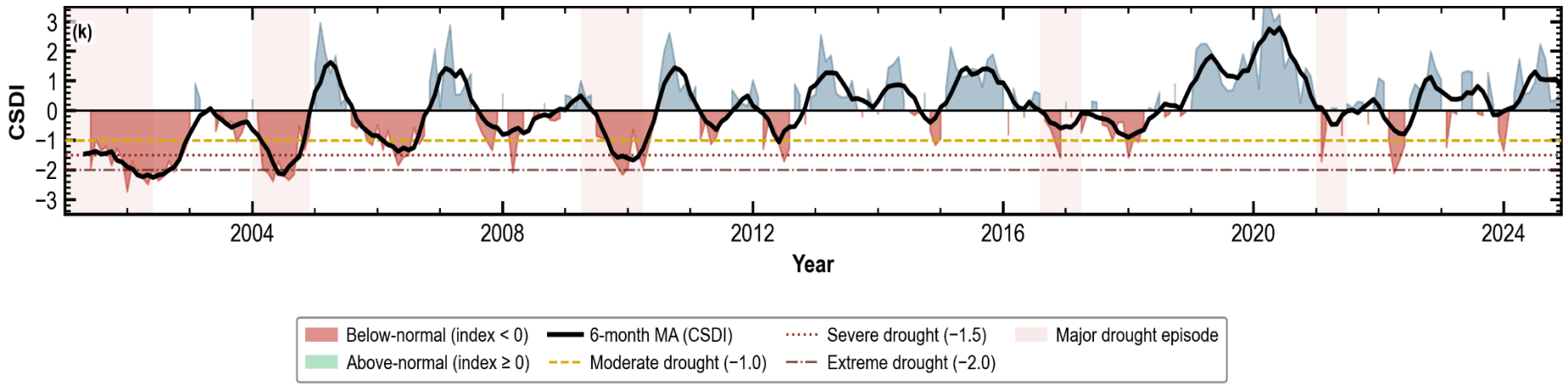
(c)


Normalised Index (z-score)
Moderate
Severe
Extreme
SPEI-3
SPEI-6
SPEI-12
2000
2004
2008
2012
2016
2020
2024

(d)


RAI (KPK Spatial Mean)
Moderate Wet
Moderate Dry
Severe Dry
Dry anomaly
Wet anomaly
Date
2000
2004
2008
2012
2016
2020
2024

(e)



(f)

Figure 6: (a) Pearson correlation matrix for nine drought indices and z-score normalised time series of all indices from 2001 to 2024 for (b) Vegetative indices (c) SPI (d) SPEI (e) time series for RAI anomaly where blue shows wet anomaly and brown shows dry anomaly, and finally (f) showing the CSDI time series with specific thresholds.

3.6 Seasonal Drought Structure

The seasonal mean area CSDI graphs in Figure 7 demonstrate that the monsoon season JJA consistently produces the most favorable moisture conditions across the province (CSDI values more than 0, while the premonsoon MAM season is the most drought vulnerable, with mean CSDI less than −0.5 across the southern and central districts. The winter DJF season shows near normal conditions in most years but with notable variability in northern districts where snowfall delivery is strongly modulated by the El Niño Southern Oscillation (ENSO) and the North Atlantic Oscillation (NAO). The premonsoon season sustains the highest mean drought area 28.4% of KPK on average, followed by the post monsoon with 21.3%, winter 19.8%, and monsoon 14.7%.

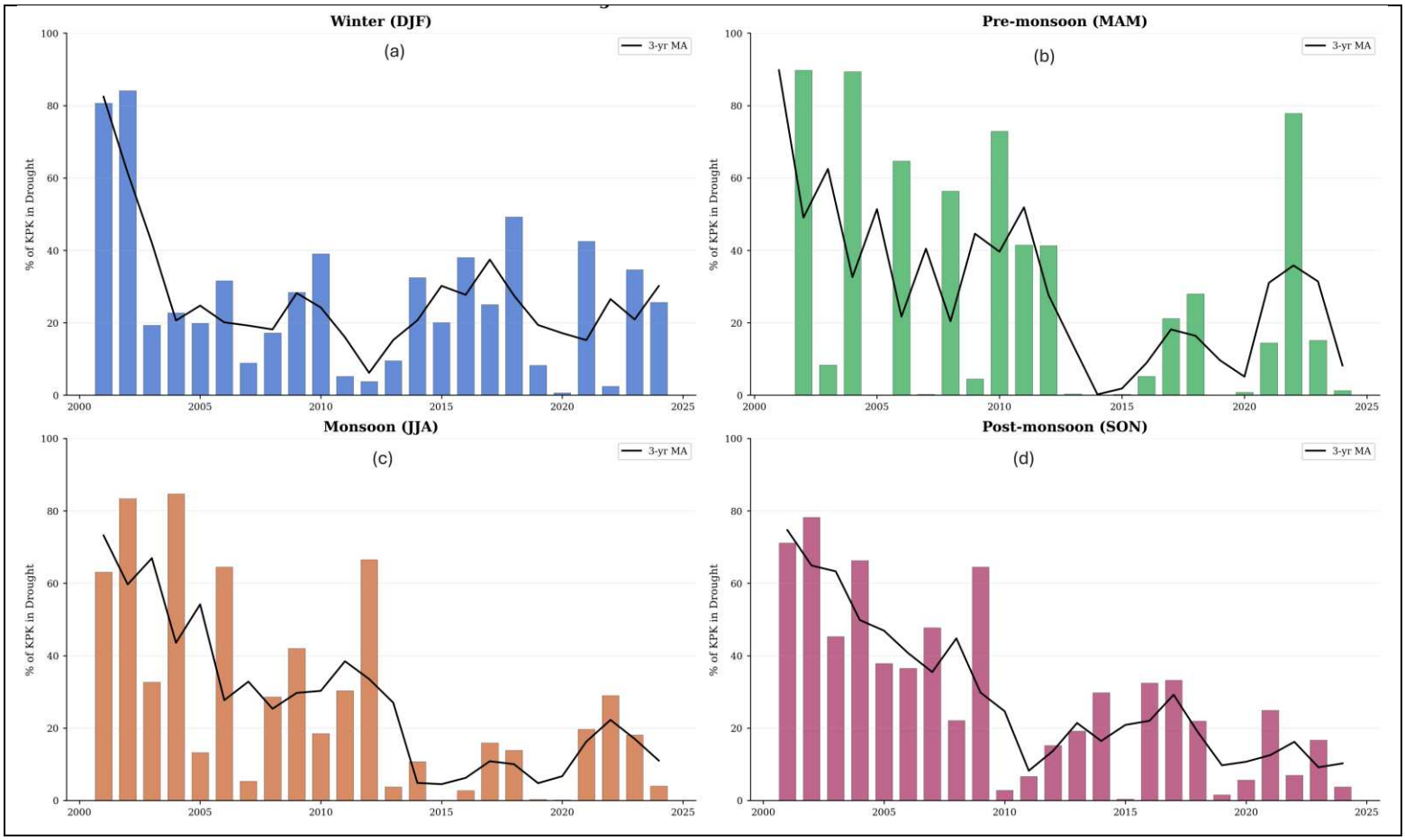


Figure 7: Seasonal mean CSDI spatial patterns for KPK from 2001 to 2024 with (a) Winter (DJF) (b) Pre-monsoon (MAM) (c) Monsoon (JJA) and (d) Post-monsoon (SON).

3.7 Decadal CSDI Anomaly Shifts

The decadal CSDI anomaly maps in Figure 8 reveal a distinct three phase structure in the province's long term drought trajectory. The first decade 2001 to 2010 was dominated by negative anomalies across most of the province, driven by the 2001 to 2002 multi year drought and the 2004 and 2009 to 2010 period, which are the three most spread events in the record. The 2011 to 2020 decade shows near normal to slightly positive anomalies across the central and northern districts, disrupted by the 2016 to 2017 episode in the south, reflecting an overall improvement in moisture conditions relative to the drought dominated first decade. The most recent sub period 2021 to 2024 shows a return to negative anomalies in the southern lowlands, consistent with the 2021 drought episode and the statistically significant drying trend. The northern districts maintain near neutral to positive anomalies throughout all three periods, reinforcing the north south deviation in drought trajectory.

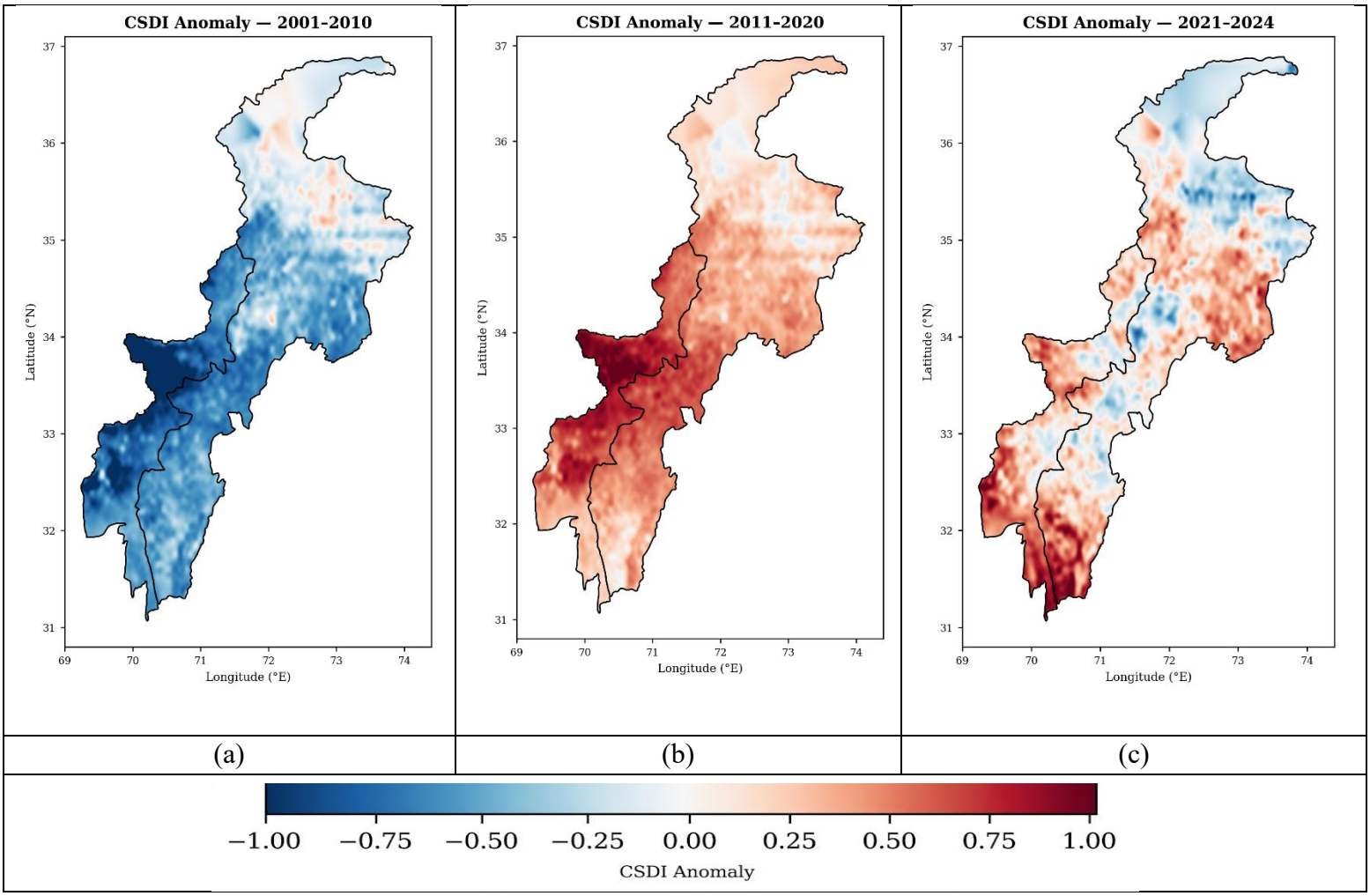


Figure 8: Decadal CSDI anomaly maps relative to 2001 to 2024 baseline mean including (a) 2001 to 2010 (b) 2011 to 2020 and (c) 2021 to 2024.

3.8 Rainfall Anomaly Index (RAI)

Figure 9 presents the spatial distribution of annual RAI values for representative years. The RAI provides a validation of the CSDI's drought identification, relying on no distributional assumptions beyond the ordering of the historical record. The five most negative RAI years, RAI in 2002 was −2.43, in 2004 it is −2.16, in 2006 value is −1.67, in 2009 its −1.89 and in 2022 it is −1.76, and the closely match the CSDI identified drought years, confirming the consistency of the composite. Spatial RAI maps reveal that the southern districts consistently show the most strongly negative annual anomalies, while Chitral and Dir in the extreme north occasionally display positive RAI even in drought years attributable to the partial decoupling of northern winter precipitation from the monsoon system that drives southern KPK precipitation (Hussain et al., 2021; Wester et al., 2019). (Khan et al., 2020) states that Chitral, Drosh and Pattan which are meteorological stations within the Hindukush region experienced a positive trend of variability, while Dir and Saidu Sharif were exceptions suggesting a near neutral or negative trend for Dir in annual variability.

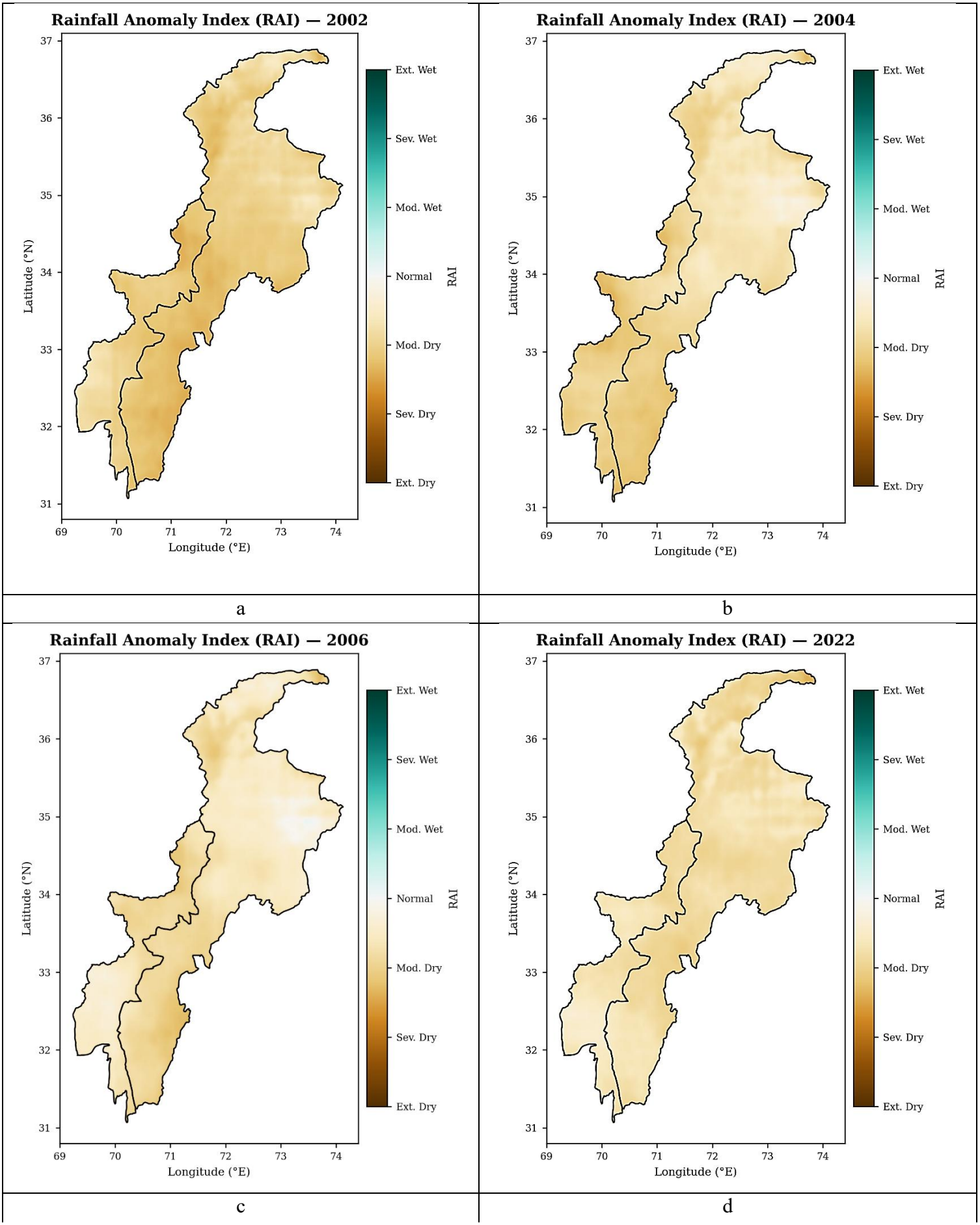
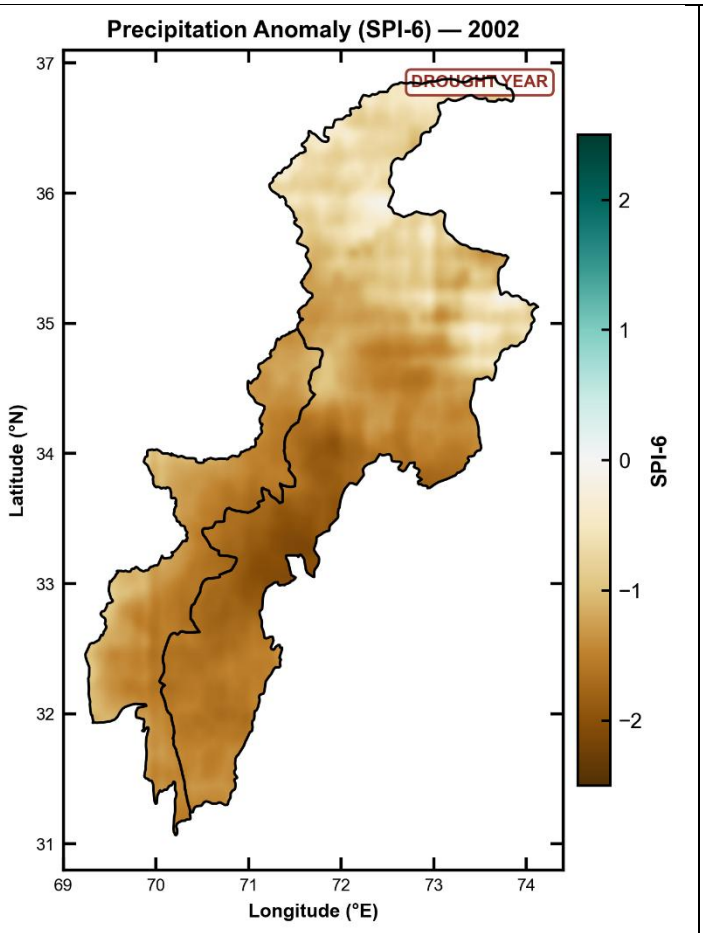
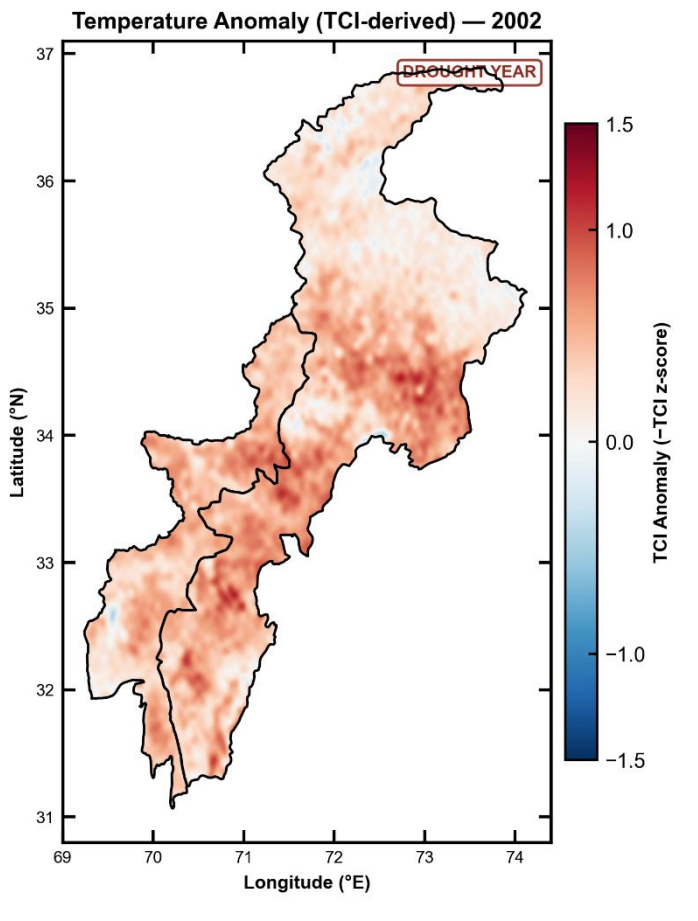


Figure 9: Annual mean Rainfall Anomaly Index (RAI) for representative years for significant years including (a) 2002 (b) 2004 (c) 2006 and (d) 2022. Blue tones indicate above normal precipitation and red tones indicate deficits.

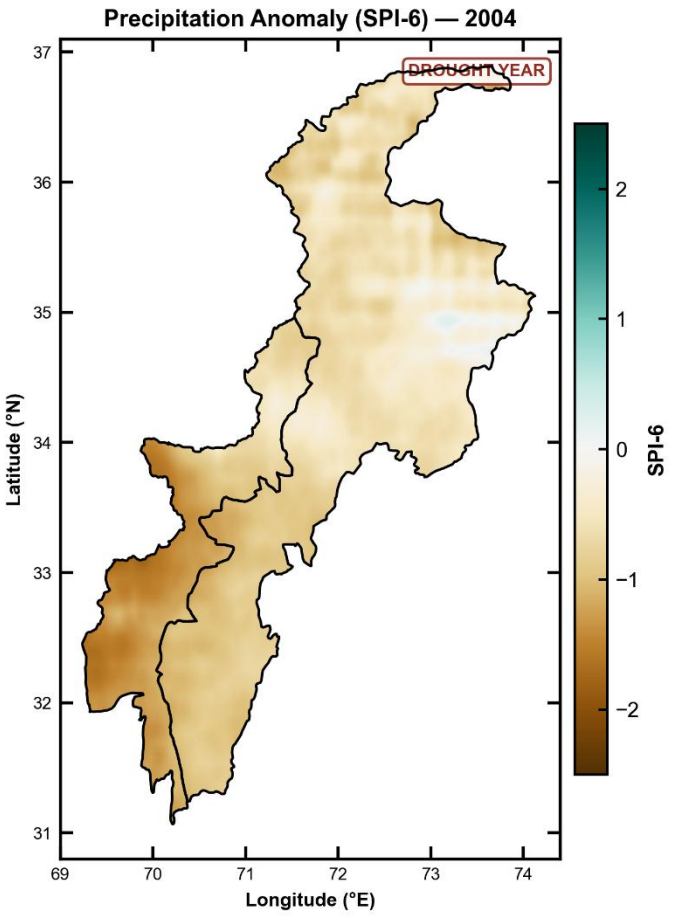
Figure 10 presents annual maps of CHIRPS precipitation anomaly and MODIS land surface temperature anomaly for the major drought years. The maps reveal that precipitation deficits and positive temperature anomalies are not uniformly located across the province. During the 2002 drought, precipitation deficits are most extreme in the southern districts like D.I. Khan, Tank and Bannu with CHIRPS anomalies exceeding 40% of the mean, while the northern districts show near normal to slightly negative anomalies. Positive LST anomalies are concentrated in the southern and central lowlands amplifying evaporative demand precisely where precipitation is most deficient, a compound spatial pattern that explains the exceptional CSDI decline of that year. The 2004 episode displays a similar spatial structure but with the precipitation shortage centered further into the central Peshawar. During 2009 to 2010, the shortage is more diffuse but sustained across two consecutive monsoon seasons. Notably, the northern districts of Chitral and Dir show near neutral to positive precipitation anomalies even in years where the south experiences severe deficits, confirming the orographic dissociating between the monsoon fed south and the westerly fed north. The temperature anomaly maps for 2016 and 2021 show positive LST across the entire province regardless of precipitation status, consistent with the broad warming trend over the HKH region documented by (Shrestha et al., 2019) and suggesting that temperature driven evaporative demand is becoming an increasingly important independent driver of drought severity independent of precipitation anomaly alone.



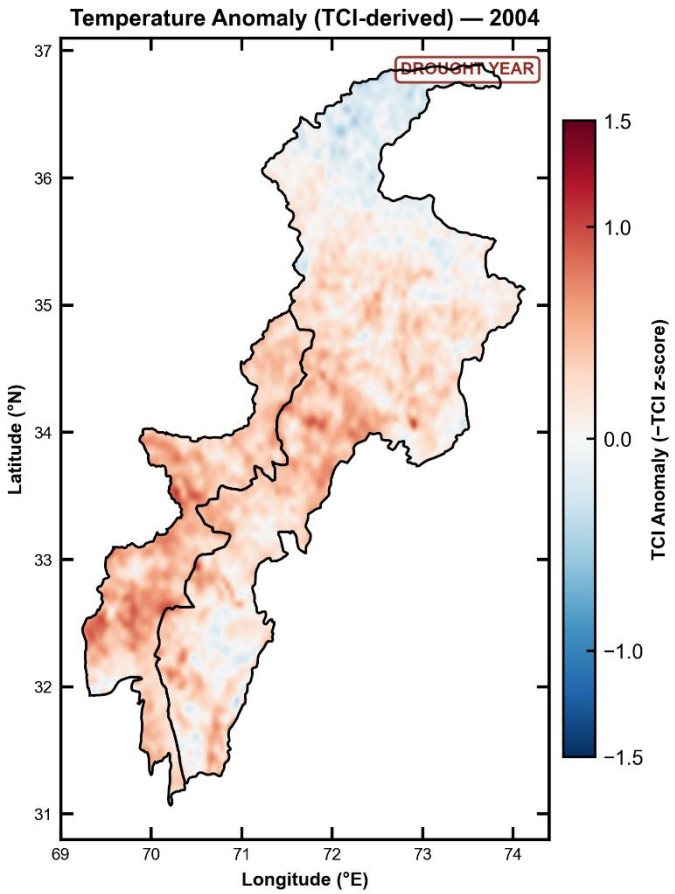
a



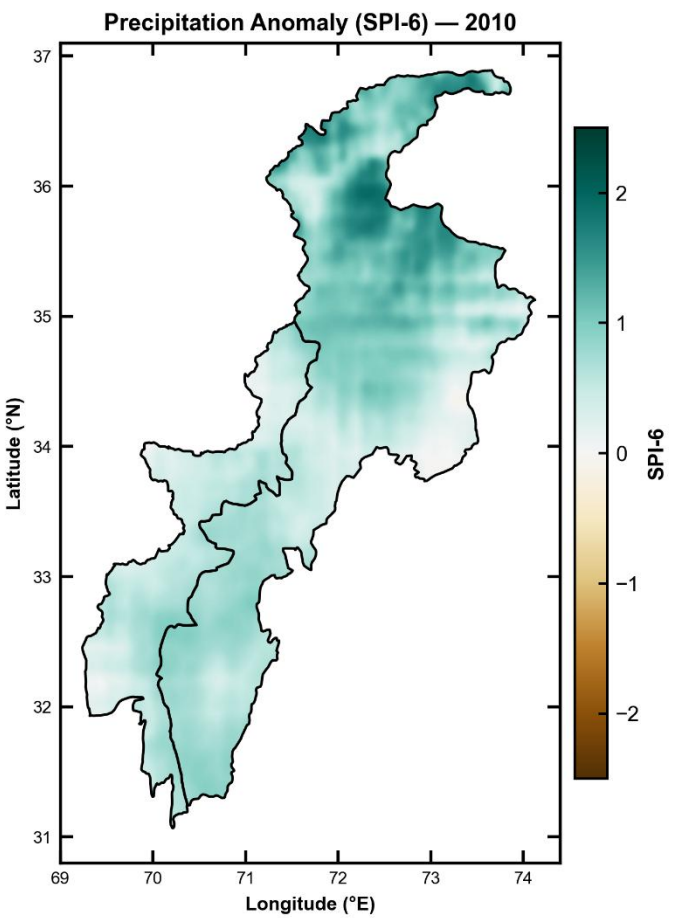
b


Precipitation Anomaly (SPI-6) — 2004
DROUGHT YEAR
Latitude (°N)
Longitude (°E)
SPI-6

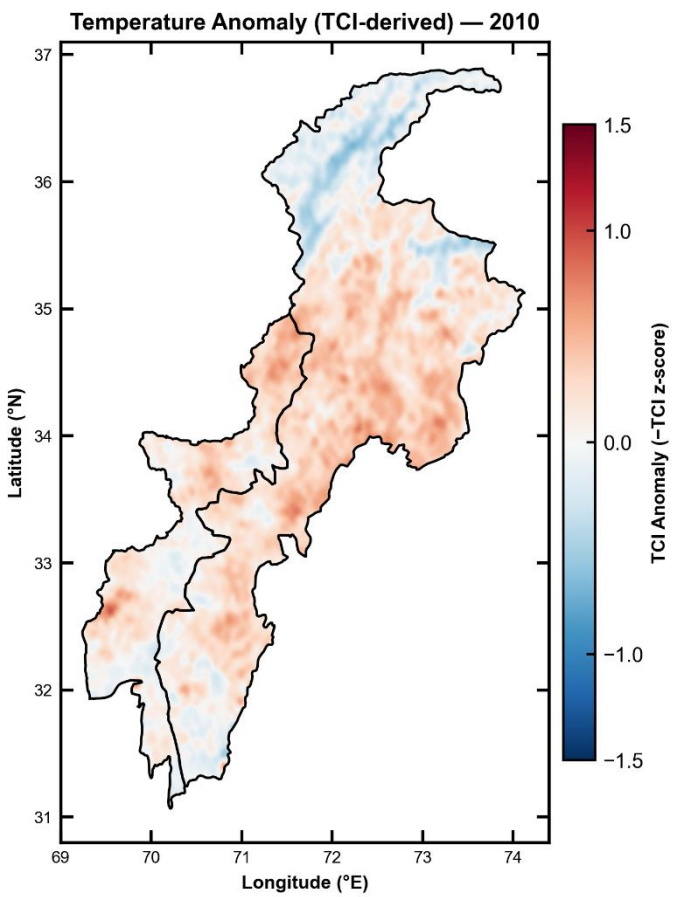
c


Temperature Anomaly (TCI-derived) — 2004
DROUGHT YEAR
Latitude (°N)
Longitude (°E)
TCI Anomaly (−TCI z-score)

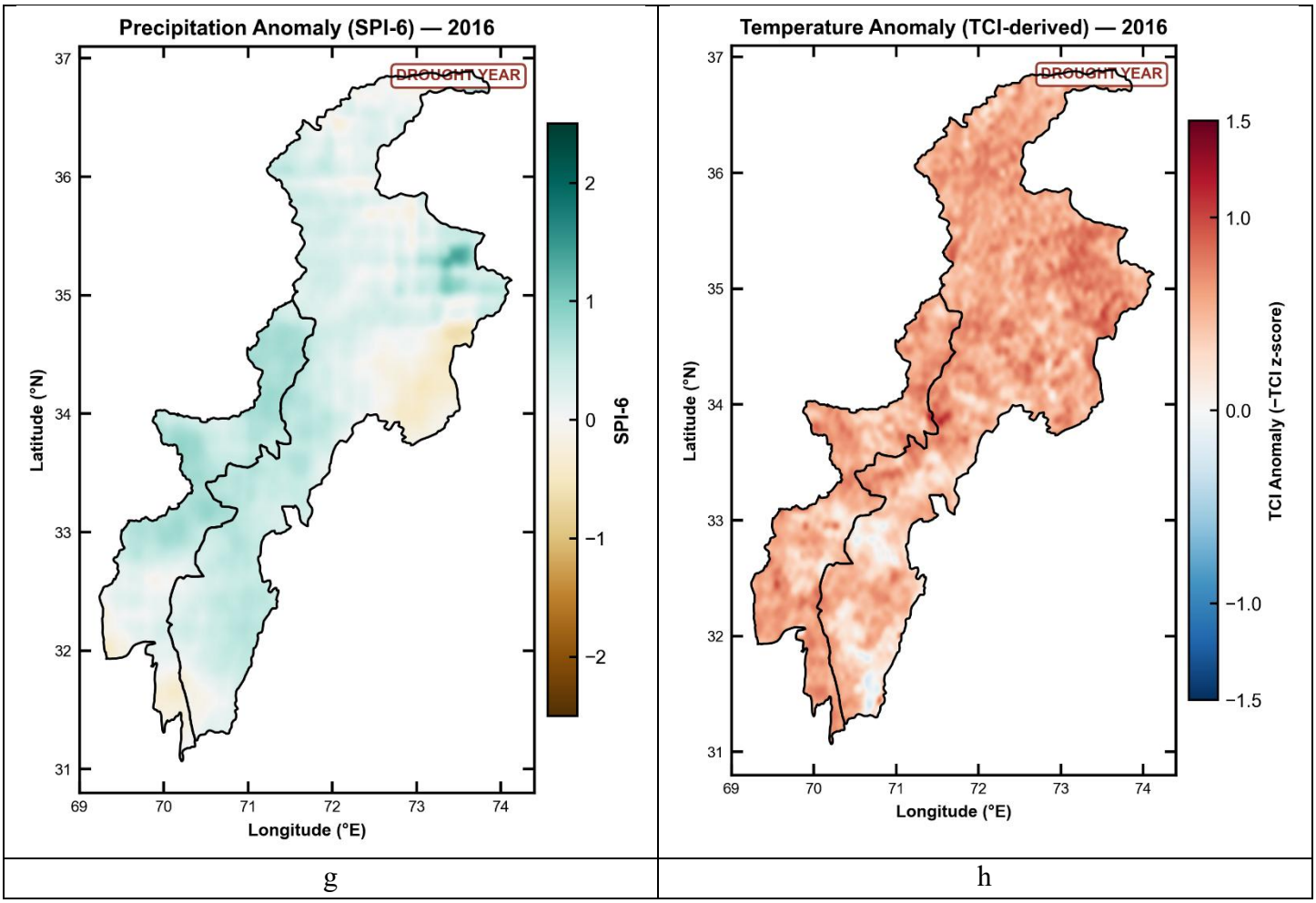
d


Precipitation Anomaly (SPI-6) — 2010
Latitude (°N)
Longitude (°E)
SPI-6

e


Temperature Anomaly (TCI-derived) — 2010
Latitude (°N)
Longitude (°E)
TCI Anomaly (−TCI z-score)

f



g h

Figure 10: Annual spatial maps of CHIRPS precipitation anomaly for percentage departure from mean value for (a) 2002 (c) 2004, (e) 2010 and (g) 2016 and MODIS land surface temperature anomaly in °C for (b) 2002, (d) 2004, (f) 2010, and (h) 2016 as the major drought years.

4. Discussion

The multi index composite approach adopted here captures dimensions of the drought cycle that no single index can represent alone. The moderate but meaningful deviation between SPI and SPEI particularly during the post 2010 warming years demonstrates that rising temperatures are increasing atmospheric moisture demand in KPK above and beyond what precipitation deficits alone would produce. This pattern is consistent with the accelerated warming documented across the HKH region by (Shrestha et al., 2019) and (Wester et al. 2019) and aligns with the finding of (Vicente Serrano et al., 2010) that the divergence between SPI and SPEI is a strong indicator of temperature forced drought intensification. The lower correlation between ESI and precipitation based indices is consistent with global analyses showing that ESI responds to root zone soil moisture depletion and vapor pressure deficit dynamics that are poorly captured by precipitation records alone (Shahzaman et al., 2021; Aghakouchak et al., 2021).

Drought trends in KPK are not spatially uniform. 63.8% of pixels show significant trends, with the majority positive wetting rather than negative drying. This result must not be misread as evidence that KPK is uniformly becoming wetter. The positive trends are concentrated in northern mountainous districts where westerly driven winter precipitation appears to have slightly increased, consistent with the broader Karakoram Anomaly pattern documented by (Wester et al., 2019). The drought risk story lies specifically in the significant negative trends in the southern lowlands like D.I. Khan, Tank, Bannu and Lakki Marwat where the drying is concentrated in the Rabi season and is already covered on a background of high drought frequency i.e. 2.1 to 2.7 events per year and long event durations i.e. 5 to 7 months per event. This

spatial difference has direct policy implications. Drought adaptation investments should be geographically targeted at the southern lowlands rather than the whole province. The south north gradient in drought trend aligns with the spatial structure identified by (Adnan et al., 2018) and (Khan et al., 2021) using station based SPI, but the present study's pixel level satellite approach reveals its spatial complexity at a resolution not previously achievable for KPK.

The strong drying signal in the Rabi season relative to the Kharif season has significant implications for winter wheat production. Rabi wheat is the dominant cereal crop across the central and southern districts, accounting for approximately 60% of provincial cereal output. Its critical growth stages include development (October to November) and grain filling (February to March) fall precisely in the months of greatest drying trend when soil moisture recharges from winter precipitation is declining most rapidly. The RAI analysis independently confirms this Rabi season precipitation deficit pattern. In contrast, the Kharif season shows mixed or neutral trends in most districts, suggesting that monsoon delivery has not systematically declined, though its interannual variability remains high. The premonsoon season shows the highest mean drought area and the tightest compound driver relationship between precipitation deficit and high LST which is the same season that also hosts the harvest and land preparation cycle making it the period of greatest compound agricultural risk.

This study relies exclusively on satellite and reanalysis products without independent ground validation from rain gauge or soil moisture records. This limitation is inherent to the sparse environment of KPK and is explicitly acknowledged. However, three lines of evidence support the credibility of the results in the absence of ground data. First, the physical consistency across nine independent products derived from three separate observational systems provides multisource cross validation. Convergent identification of the same drought episodes by SPI, MODIS VCI, and SPEI is unlikely to reflect a common systematic bias. Second, the five major drought episodes identified by the CSDI 2001 to 2002, 2004, 2009 to 2010, 2016 to 2017, and 2021 are each independently documented in the peer reviewed literature for Pakistan, providing literature based event level validation (Rahman et al., 2018; Rahman et al., 2021; Rahman et al., 2022). Third, the CHIRPS product used for SPI and RAI computation has been independently validated against Pakistan rain gauge records and demonstrated to outperform alternative gridded products over the complex terrain of the HKH (Iqbal et al., 2021). The Thornthwaite PET method used for SPEI likely underestimates PET under high vapor pressure deficit conditions relative to the Penman Monteith formulation, suggesting that the SPEI drought intensities reported here may slightly underestimate the true atmospheric demand component. Future work integrating GRACE, GRACE-FO Total Water Storage Anomaly data and streamflow records from the Indus River System Authority gauge network would provide direct hydrological cross-validation of the CSDI product.

5. Conclusion

This study presented a fully satellite driven, multi index drought monitoring and projection framework for Khyber Pakhtunkhwa, Pakistan, operating at 0.05° spatial resolution and monthly temporal resolution for the period 2001 to 2024, with future projections extending to 2100.

Nine drought indices including SPI 3,6,12, SPEI 3,6,12, VCI, TCI, and ESI were successfully integrated via Principal Component Analysis into a Composite Drought Severity Index that captures the multidimensional character of drought more comprehensively than any single index. The first principal component explained the dominant shared variance across all index families, confirming the physical coherence of the composite.

Five major drought episodes were identified over the study period, with the 2001 to 2002 event affecting over 63% of provincial areas which is the most spatially extensive drought in the 24 year record. The southern lowland districts of D.I. Khan, Tank, Bannu, and Lakki Marwat consistently show the highest drought frequency, longest durations, and greatest percentage of time classified under drought conditions.

Mann Kendall trend analysis detected statistically significant drying trends in the southern and central districts of KPK, concentrated particularly during the Rabi (October to March) season. The northern mountainous districts show neutral to weakly positive trends, suggesting a north south divergence in drought trajectory that reflects contrasting responses to monsoon variability versus westerly driven winter precipitation.

These results provide the first spatially explicit, multi index, satellite derived drought climatology dataset for KPK at the sub district spatial scale. The framework requires no in-situ validation data and is directly transferable to other data-sparse provinces across the Hindu Kush Himalaya region.

Declarations

Conflict of Interest

The authors declare no competing financial interests or personal relationships that could have influenced the work reported in this paper.

Funding

This study received no specific grant from any public, commercial, or not-for-profit funding agency.

Data Availability Statement

All satellite data used in this study are publicly available. CHIRPS v2.0 precipitation data are available from the Climate Hazards Center at https://www.chc.ucsb.edu/data/chirps. MODIS MOD13A3, MOD11A2, and MOD16A2 products are available from the NASA Earthdata portal (https://earthdata.nasa.gov) and the Google Earth Engine data catalog. ERA5-Land reanalysis data are available from the Copernicus Climate Data Store (https://cds.climate.copernicus.eu). Derived drought index NetCDF files and analysis scripts are available from the corresponding author upon reasonable request.

CRediT Authorship Contribution Statement

- Farjad Aziz: Conceptualization, Methodology,
- Muhammad Waseem: Supervision, Formal Analysis.
- Zeeshan Asghar: Conceptualization, Modelling
- Faisal Baig: Data Curation and Investigation
- Waqas Arshad Tanoli: Visualization, Writing

AI Disclosure

All data acquisition, processing, index computation, statistical analysis, figure generation, and scientific interpretation were performed by the authors. No AI-generated text was incorporated into the results, methods, or conclusions sections without expert human review and validation.

Ethical Statement

This study is based exclusively on publicly available remote sensing and reanalysis datasets and did not involve human subjects, animal experiments, or sensitive personal data. Formal ethical approval was therefore not required.

References

Adnan, S., Ullah, K., Shuanglin, L., Gao, S., Khan, A. H., & Mahmood, R. (2018). Comparison of various drought indices to monitor drought status in Pakistan. Climate Dynamics, 51(5), 1885–1899. https://doi.org/10.1007/s00382-017-3987-0

Aghakouchak, A., Farahmand, A., Melton, F. S., Teixeira, J., Anderson, M. C., Wardlow, B. D., & Hain, C. R. (2021). Remote sensing of drought: Progress, challenges and opportunities. Reviews of Geophysics, 53(2), 452–480. https://doi.org/10.1002/2014RG000456

Bhatti, M. T., Anwar, A. A., & Hussain, K. (2023). *Characterization and outlook of climatic hazards in an agricultural area of Pakistan*. Scientific Reports, 13, 10271. https://doi.org/10.1038/s41598-023-36909-4

Döscher, R., Acosta, M., Alessandri, A., Anthoni, P., Arneth, A., Arsouze, T., … Wyser, K. (2022). The EC-Earth3 Earth system model for the Coupled Model Intercomparison Project 6. Geoscientific Model Development, 15(7), 2973–3020. https://doi.org/10.5194/gmd-15-2973-2022

Funk, C., Peterson, P., Landsfeld, M., Pedreros, D., Verdin, J., Shukla, S., … Michaelsen, J. (2015). The climate hazards infrared precipitation with stations—a new environmental record for monitoring extremes. Scientific Data, 2(1), 150066. https://doi.org/10.1038/sdata.2015.66

Hao, Z., & AghaKouchak, A. (2014). A nonparametric multivariate multi-index drought monitoring framework. Journal of Hydrometeorology, 15(1), 89–101. https://doi.org/10.1175/JHM-D-12-0160.1

Haroon, M. A., Zhang, J., Yao, F., Saleem, F., Al-Hemoud, A., Shafeeque, M., Cheema, M. J. M., Bilal, M., Habib-ur-Rahman, M., & Khan, A. (2021). *Drought monitoring and performance evaluation of MODIS-based drought severity index over Pakistan*. Natural Hazards, 108(1), 759–784. https://doi.org/10.1007/s11069-016-2490-y

Hina, S., Saleem, F., Arshad, A., Hina, A., & Ullah, I. (2021). Droughts over Pakistan: possible cycles, precursors and associated mechanisms. *Geomatics, Natural Hazards and Risk*, *12*(1), 1638–1668. https://doi.org/10.1080/19475705.2021.1938703

Hu, P., Sharifi, A., Tahir, M. N., Tariq, A., Zhang, L., Mumtaz, F., & Shah, S. H. I. A. (2021). *Evaluation of vegetation indices and phenological metrics using time-series MODIS data for monitoring vegetation change in Punjab, Pakistan*. Water, 13(18), 2550. https://doi.org/10.3390/w13182550

Hussain, M. S., Lee, S., & Hussain, I. (2021). Large-scale atmospheric circulation patterns associated with extreme monsoon precipitation in Pakistan during 1981–2018. Atmospheric Research, 253, 105489. https://doi.org/10.1016/J.ATMOSRES.2021.105489

Jehan, I., Atta-ur-Rahman & Waqas, T. Assessment of meteorological drought and trend detection in Khyber Pakhtunkhwa, Pakistan. Arab J Geosci 13, 765 (2020). https://doi.org/10.1007/s12517-020-05747-3

Kendall, M. G. (1975). Rank Correlation Methods (4th ed.). Charles Griffin.

Khan, I., Waqas, T., Samiullah et al. Precipitation variability and its trend detection for monitoring of drought hazard in northern mountainous region of Pakistan. Arab J Geosci 13, 698 (2020). https://doi.org/10.1007/s12517-020-05700-4Kogan, F. N. (1995). Application of vegetation index and brightness temperature for drought detection. Advances in Space Research, 15(11), 91–100. https://doi.org/10.1016/0273-1177(95)00079-T

Mann, H. B. (1945). Nonparametric tests against trend. Econometrica, 13(3), 245–259. https://doi.org/10.2307/1907187

McKee, T. B., Doesken, N. J., & Kleist, J. (1993). The relationship of drought frequency and duration to time scales. Proceedings of the 8th Conference on Applied Climatology, 17–22 January 1993, Anaheim, CA, USA, pp. 179–183.

Mishra, A. K., & Singh, V. P. (2010). A review of drought concepts. Journal of Hydrology, 391(1–2), 202–216. https://doi.org/10.1016/j.jhydrol.2010.07.012

Moazzam, M. F. U., Rahman, G., Munawar, S., Tariq, A., Safdar, Q., & Lee, B.-G. (2022). *Trends of rainfall variability and drought monitoring using standardized precipitation index in a scarcely gauged basin of northern Pakistan*. Water, 14(7), 1132. https://doi.org/10.3390/w14071132

Müller, W. A., Jungclaus, J. H., Mauritsen, T., Baehr, J., Bittner, M., Budich, R., … Marotzke, J. (2018). A higher-resolution version of the Max Planck Institute Earth System Model (MPI-ESM1.2-HR). Journal of Advances in Modeling Earth Systems, 10(7), 1383–1413. https://doi.org/10.1029/2017MS001217

Muñoz-Sabater, J., Dutra, E., Agustí-Panareda, A., Albergel, C., Arduini, G., Balsamo, G., … Thépaut, J.-N. (2021). ERA5-Land: A state-of-the-art global reanalysis dataset for land applications. Earth System Science Data, 13(9), 4349–4383. https://doi.org/10.5194/essd-13-4349-2021

Rahman, G., Rahman, A.-u., Ullah, S., Dawood, M., Moazzam, M. F. U., & Lee, B. G. (2021). *Spatio-temporal characteristics of meteorological drought in Khyber Pakhtunkhwa, Pakistan*. PLOS ONE, 16(4), e0249718. https://doi.org/10.1371/journal.pone.0249718

Rahman, G., Rahman, A.-u., Samiullah, & Dawood, M. (2018). *Spatial and temporal variation of rainfall and drought in Khyber Pakhtunkhwa Province of Pakistan during 1971–2015*. Arabian Journal of Geosciences, 11, 46. https://doi.org/10.1007/s12517-018-3396-7

Rahman, G., Rahman, A.-u., Anwar, M. M., Dawood, M., & Miandad, M. (2022). *Spatio-temporal analysis of climatic variability, trend detection, and drought assessment in Khyber Pakhtunkhwa, Pakistan*. Arabian Journal of Geosciences, 15, 81. https://doi.org/10.1007/s12517-021-09382-4

Rahman, K. U., Shang, S., Shahid, M., & Wen, Y. (2021). Evaluating the meteorological drought characteristics over Pakistan using in situ observations and reanalysis products. International Journal of Climatology, 41(9), 4437–4458. https://doi.org/10.1002/joc.7063

Shahzaman, M., Zhu, W., Ullah, I., Mustafa, F., Bilal, M., Ishfaq, S., Nisar, S., Arshad, M., Iqbal, R., & Aslam, R. W. (2021). *Comparison of multi-year reanalysis, models, and satellite remote sensing products for agricultural drought monitoring over South Asian countries*. Remote Sensing, 13(16), 3294. https://doi.org/10.3390/rs13163294

Sen, P. K. (1968). Estimates of the regression coefficient based on Kendall's tau. Journal of the American Statistical Association, 63(324), 1379–1389. https://doi.org/10.1080/01621459.1968.10480934

Shahid, M., Rahman, K. U., Haider, S., Gabriel, H. F., Khan, A. J., Pham, Q. B., Mohammadi, B., Linh, N. T. T., & Anh, D. T. (2021). *Assessing the potential and hydrological usefulness of the CHIRPS precipitation dataset over a complex topography in Pakistan*. Hydrological Sciences Journal, 66(11), 1664–1684. https://doi.org/10.1080/02626667.2021.1957476

Shrestha, A. B., Wester, P., Mukherji, A., & Eriksson, M. (Eds.). (2019). The Hindu Kush Himalaya assessment: Mountains, climate change, sustainability and people. Springer. https://doi.org/10.1007/978-3-319-92288-1

Tatebe, H., Ogura, T., Nitta, T., Komuro, Y., Ogochi, K., Takemura, T., … Kimoto, M. (2019). Description and basic evaluation of simulated mean state, internal variability, and climate sensitivity in MIROC6. Geoscientific Model Development, 12(7), 2727–2765. https://doi.org/10.5194/gmd-12-2727-2019

Vicente-Serrano, S. M., Beguería, S., & López-Moreno, J. I. (2010). A multiscalar drought index sensitive to global warming: The Standardized Precipitation Evapotranspiration Index. Journal of Climate, 23(7), 1696–1718. https://doi.org/10.1175/2009JCLI2909.1

Wester, P., Mishra, A., Mukherji, A., & Shrestha, A. B. (2019). Unravelling climate change in the Hindu Kush Himalaya: Rapid warming in the mountains and increasing extremes. In A. B. Shrestha et al.

(Eds.), The Hindu Kush Himalaya Assessment (pp. 57–97). Springer. https://doi.org/10.1007/978-3-319-92288-1_3